NTNU
Norwegian University of
Science and Technology

Partial Discharge Detection in Power Electronic Substrates Exposed to Pulse Voltage Waveforms

Morten Lund Torkildsen

Master of Science in Electric Power Engineering
Submission date: June 2018
Supervisor: Kaveh Niayesh, IEL
Co-supervisor: Lars Lundgaard, SINTEF

Norwegian University of Science and Technology
Department of Electric Power Engineering

Problem Description

Application of semiconductor switching devices is increasing in power systems. This imposes all insulation materials to new types of voltage stresses (fast repetitive pulses), for which they are not designed and dimensioned. The previous studies show this new type of voltage stress adversely impacts the performance of the insulation systems, e.g. in form of reduced partial discharge inception voltage or accelerated ageing. Novel test techniques for such stresses needs to be developed.

The student will develop an experimental setup to investigate partial discharge in some simplified semiconductor samples, under this type of repetitive pulse voltage stress. This includes optical, acoustic and electrical detection, whereas the main focus will be put on electrical detection of partial discharges. For this purpose, appropriate measurement methods with adequately large frequency bandwidths are to be developed in order to capture the partial discharge. Furthermore, suitable techniques have to be utilized to extract the partial discharge related signal out of the measured electrical quantities by suppressing the influence of the applied voltage stress.

Preface

This master thesis has been performed at the Department of Electric Power Engineering, NTNU, Trondheim. The objective has been to create a system for detection of PD in semiconductor substrate test objects at a fast-rising square voltage.

I would like to thank my supervisor, professor Kaveh Niayesh at NTNU, and co-supervisor Lars Lundgaard at SINTEF Energy Research for their guidance and feedback throughout my work. A big thank you also goes to Erlend Grytli Tveten and Dag Linhjell at SINTEF Energy Research for their assistance when learning to use the measuring equipment, and their help with solving my various problems with the experimental setup. I would also like to thank the people at NTNUs mechanical and electrical workshops for their help when making my own measuring devices and troubleshooting the experimental setup. Finally, I would like to thank Olaf Hohlfeld at Infineon for his motivating interest in the project.

Trondheim, June 2018

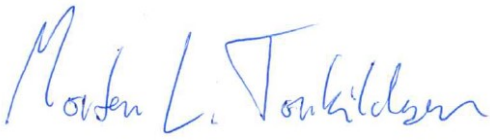

Morten Lund Torkildsen

Abstract

An increasing number of power electronic converters are integrated in power systems. The fundamental functionality of electronic converters is turning on and off semiconductor switches to form the wanted voltage shape. This causes fast repetitive voltage pulses which can have negative effects on the insulation systems. The increased degradation of the insulation systems is due to several mechanisms, but partial discharges (PD) is considered most harmful. The insulation of the electronic converter itself is also vulnerable to PD. Today, power electronic devices are tested for PD when the system voltage is above a certain level. They are not tested with the pulsed voltages they are exposed to, but rather using a conventional method applying a sinusoidal voltage. The conventional method for PD detection is unsuited for pulsed voltage conditions, and new detection methods must be developed.

The objective for this project has been to create a system for detection of PD in semiconductor substrate test objects at a fast-rising square voltage. The current through the test objects has been investigated using a frequency analyzer to identify the frequency content of the applied voltage and PD pulses. Three different interfaces for measuring the current through the test object has been made for direct, inductive and electromagnetic measurements respectively; resistive shunt, high frequency current transformer (HFCT) and antenna. Three different methods of suppressing the influence of the applied voltage has also been tested; filter, wavelet analysis and subtraction by average.

A functioning PD measuring system has been made utilizing a standard oscilloscope connected to a computer with Matlab for data collection. Current measurements were done using the resistive shunt. A Matlab script was made to suppress the influence of the applied voltage using the subtraction by average method. This script was also used to extract and plot the amplitude and location of the detected PD pulses. Optical detection with a photomultiplier was utilized as a method of confirming the electrical measurements.

Sammendrag

Bruken av kraftelektronikkomformere er økende i kraftsystemet. Den grunnleggende funksjonen til kraftelektronikkomformere er å skru av og på halvlederbrytere for å oppnå den ønskede spenningsformen. Dette fører til raske, repeterende spenningspulser som kan ha en negativ effekt på isolasjonssystemene. Den økte nedbrytningen av isolasjonssystemene er forårsaket av flere mekanismer, men delutladninger regnes som den mest skadelige mekanismen. Isolasjonen til kraftelektronikkomformerne er også sårbar for delutladninger. I dag testes omformere for delutladninger når spenningen er over et visst nivå. De blir ikke testet ved den type spenning de er utsatt for, men på den konvensjonelle måten med en påtrykt sinusspenning. Den konvensjonelle måten som er brukt for å teste etter delutladninger er uegnet for bruk ved repeterende spenningspulser, og nye metoder må utvikles.

Målet for dette prosjektet har vært å lage et system for deteksjon av delutladninger i halvleder-substrater ved pulsspenninger. Strømmen gjennom testobjektene har blitt undersøkt ved hjelp av en frekvensanalysator for å finne frekvensinnholdet til den påtrykte pulsspenningen og for delutladningene. Tre forskjellige grensesnitt for måling av strømmen gjennom testobjektene har blitt laget for henholdsvis direkte, induktiv og elektromagnetisk måling; resistiv shunt, høyfrekvent strømtrafo og antenne. Tre forskjellige måter å undertrykke påvirkningen fra den påtrykte spenningen er også testet; filter, wavelet analyse og korreksjon for gjennomsnitt.

Et fungerende system har blitt laget hvor en resistiv shunt ble valgt brukt for strømmåling, og korreksjon for gjennomsnitt ble valgt for å undertrykke støy. Et ordinært oscilloskop koblet opp mot en datamaskin med Matlab ble brukt for å samle inn data. Matlab ble også brukt for å prosessere dataene, først ved korreksjon for gjennomsnitt, deretter for å søke etter og plotte amplituder og plassering av delutladningene. Optisk deteksjon av delutladningene ble brukt for kontroll av de elektriske målingene.

Table of Contents

1 INTRODUCTION

An increasing number of power electronic converters are integrated in power systems. In this introduction, an overview is given on; the origin of these converters, what kind of voltages they produce and what effect they have on the insulation system. The focus is on the effects on the insulation of power electronic converters themselves, not other types of equipment in the power system. One of these effects, partial discharges (PD), is influenced by the shape of the voltage. How the converters are tested for PD today, and why this might not be the best method is also discussed.

1.1 Power Electronic Converters in the Grid

During the last years, use of power electronic converters in the grid has increased, and it is believed that the increase will be even larger in the years to come. Power electronic converters are used in e.g. motor/generator drive systems, renewable energy integration and high voltage direct current (HVDC) supply. Integration of renewable energy is a large part of this increase, a graph showing the last years' development of global capacity from wind and solar (PV) power can be seen in Figure 1.

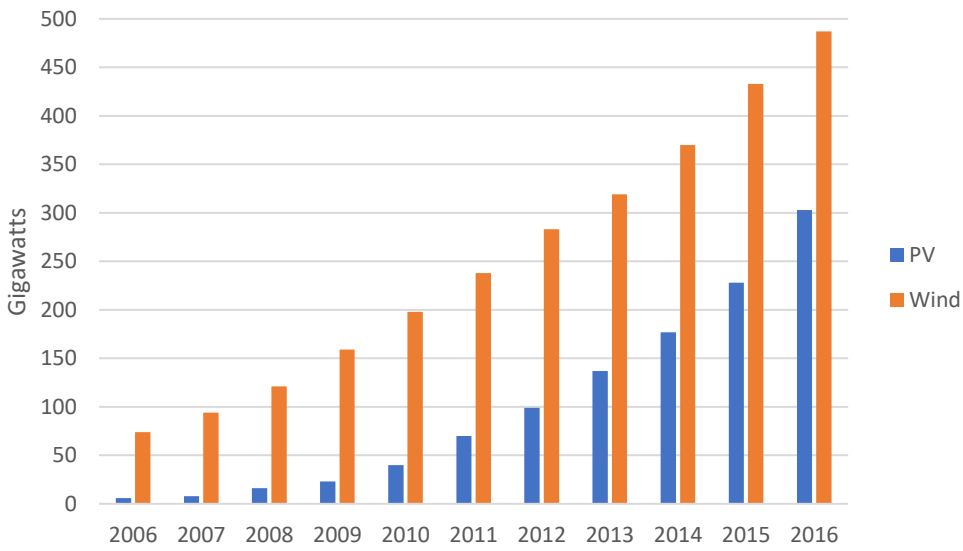

Figure 1 Wind and PV power global capacity, modified from [1].

1.2 Fast Repetitive Pulses

The fundamental functionality of power electronic converters is turning on and off semiconductor switches to form the wanted voltage shape. Converters are commonly based on transistor technology such as MOSFETs and IGBTs [2]. Considering the inverter as an example, a 50 Hz pulse width modulated (PWM) signal is formed by a carrier wave with a very high frequency together with a 50 Hz modulation wave as seen in Figure 2.

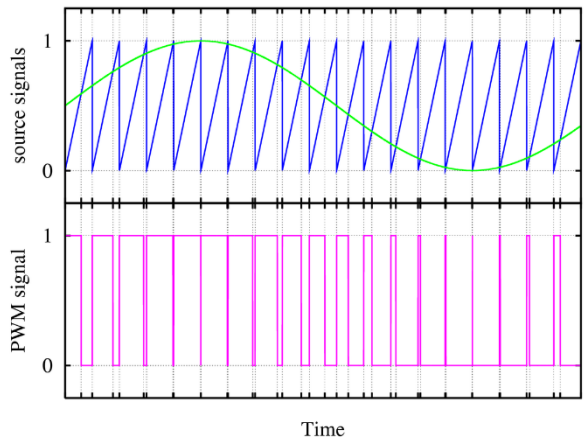

Figure 2 Simple inverter signal generation, carrier wave (blue), modulation wave (green), PWM signal (purple) [3].

These fast repetitive voltage pulses created by the power electronic converters can be described with the parameters magnitude, pulse shape and repetition rate. The pulse shape will vary depending on factors such as impedance and type of equipment and resonance in the power system. At the terminals of a motor or generator, the pulse can be shaped as seen in Figure 3. The maximum peak voltage (U_p) is reached because of a voltage overshoot (U_b) from the steady state magnitude (U_a) of the voltage pulse. Rise time is defined as the time from 10 % to 90 % of the peak voltage [4]. This voltage overshoot is due to impedance of the motor or generator supply cable and is not present at the power electronic converters.

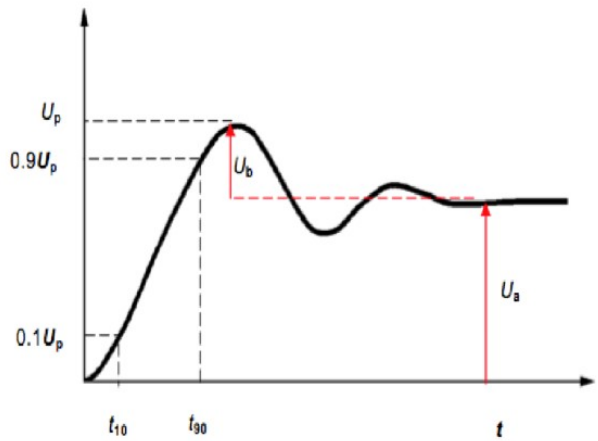

Figure 3 Front of voltage pulse, from [4].

1.3 Effect of Repetitive Pulses on Insulation

Repetitive pulses cause increased degradation of the insulation system due to i.e. intrinsic aging, space charges, treeing and partial discharges (PD), where PD generally is the most harmful mechanism [4].

Silicone gel is the preferred material used to encapsulate power electronic converters, this is because the gel has good mechanical, thermal and electrical properties. With the increasing operating voltages of converters, it leads to higher stress on the electrical insulation which can result in partial discharges (PD) [5]. Impulse voltages have been shown to cause cavities and streamer discharges in silicone gel. It has also been shown that there is a difference in degradation depending on the repetition rate of the pulses. Self-healing is observed after a short time if one voltage impulse is applied, and permanent degradation is observed if a series of impulses is applied [6].

Compared to a sinusoidal voltage, more PD activity is seen with a repetitive pulse voltage [7]. Several examples from earlier research show that the properties of the repetitive voltage affect the PD behavior [8-11]. Shorter rise time results in fewer PDs with higher magnitudes, and that the PD pulses are localized closer to the voltage flanks. A higher repetition frequency results in a lower inception voltage. Unipolar and bipolar voltage pulses are believed to have an equal effect on PD quantity and magnitude [4].

PD has been found to occur at both the rising and falling flank of impulse voltages [12] and unipolar pulsed voltages [11]. The discharges on the falling flank is due to the insulation material being charged during the rising flank making it the opposite polarity of the electrode at the falling flank. This has been seen both at solid surfaces [12] and in liquids [13].

1.4 PD Testing of Power Electronics

In power electronic converters the semiconductor switches are placed on an insulating surface called substrate. It has been shown that on these substrates, a very high local field is located in what can be called the "triple region" [14]. This is where the substrate meets both the metallization and the surrounding insulation material (silicone gel), as seen in Figure 4. The high field is caused by the differences in permittivity between substrate and silicone gel [15] and the sharp edge of the copper plates. This field may become large enough to cause PD if exposed to severe voltage conditions [14].

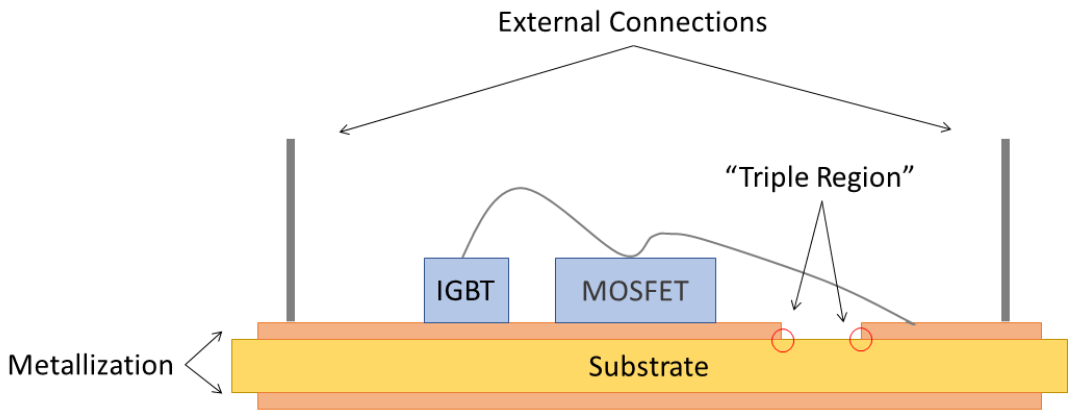

Figure 4 Illustration of power electronic substrate with semiconductor devices and connections.

Power electronic converters, such as the one illustrated in Figure 4, are tested for PD when the system voltage is above a certain level. All external connections are then short circuited, and the test voltage is applied to the base plate. The modules are tested according to IEC 60270, which means they are tested with a sinusoidal voltage [5, 15].

A sinusoidal voltage is, as seen in the previous chapters, not an accurate representation of the voltage these devices are exposed to. It has also been shown that the pulsed voltages may impact the PD properties. Based on this, it seems that PD measurements should be performed at voltages with characteristics similar to the voltage the devices are exposed to, and not exclusively with sinusoidal voltages.

1.5 Structure of the Report

The objective of this project has been to:

- Analyze the frequency content of the applied voltage and PD pulses.
- Create a measuring system for detection of PD during a fast-rising square voltage.
- Use the system to measure PD in power electronic substrate test objects.

An optical method has been used successfully in a pre-project to detect PD and is used as a verification of the PD measurements done here.

In chapter 2, theory is presented on some techniques, equipment and noise suppression proposed in literature and earlier research. The test objects, voltage source, measurement system and measuring procedure is presented in chapter 3. The results of both the frequency measurements and PD measurements is presented and discussed in chapter 4. In chapter 5 the conclusions and suggestions for further work are given.

2 PD DETECTION TECHNIQUES

The problem with measuring PD at voltages with short rise and fall times is that the high dV/dt cause the frequency spectra of the applied voltage and PDs to overlap as seen in Figure 5. Conventional PD detection is, as seen in Figure 5, also performed in the same frequency range as the applied voltage. Separating the current pulses originating from PDs, from the current pulses produced by the switching of the applied voltage is then difficult. This makes conventional detection unsuited for this task, and other detection methods must be used [8].

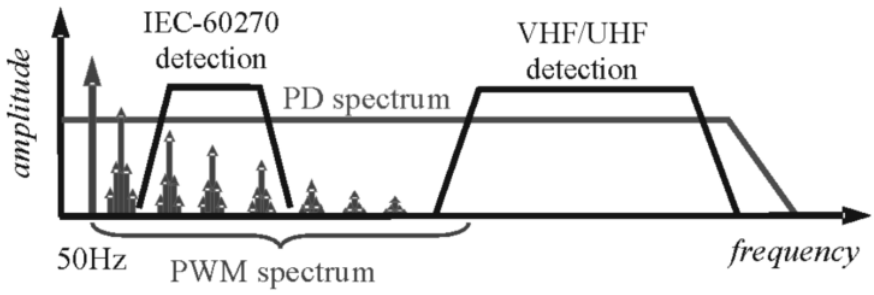

Figure 5 Applied voltage (PWM), PD and detection method spectra, from [8].

IEC/TS 61934 [16] is a technical specification of PD measurement at repetitive pulsed voltage stress. The use of electrical or electromagnetic interfaces between the test object and the measuring equipment is suggested. It also addresses the need to suppress the applied voltage. Other proposed methods include optical and acoustic detection.

2.1 Electrical Measurements

Different techniques have been used in earlier research to measure PD electrically at pulsed voltages. Some examples are; direct measurement with a 50 Ω resistance between the test object and the measurement system [17], capacitive decoupling of PD signals [18, 19] and using a high frequency current transformer (HFCT) either in a differential setup [19, 20], or measuring at the earth side of the test object [21].

2.1.1 Resistive Shunt

The following theory on resistive shunts is collected from Hauschild et al. [22]. Due to the short rise/fall times of the applied voltage, high current pulses will occur in the test object. Resistive shunts can be used to reduce this down to a measurable level. When converting high impulse currents for measurement, the resistance must be very low (mΩ range). In this case, the inductance of the circuit can have a large influence on the resulting impedance. This inductance has two origins: The inductive loop created by the connections between the measuring cable and the resistive shunt, blue area seen in Figure 6a. As well as the self-inductance of the resistive shunt. A design principle of a low-inductive shunt can be seen in Figure 6b. This will minimize the measuring error by making the inductive loop very small.

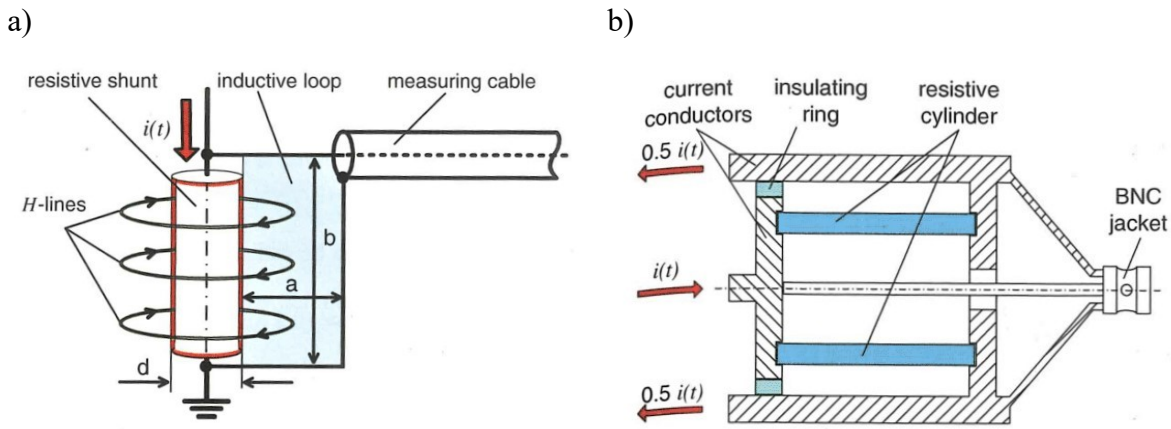

Figure 6 a Equivalent circuit showing the inductive loop **b** Design principle of low-inductive shunt, both from [22].

2.1.2 Capacitive PD coupler

Capacitive PD couplers are commonly used in conjunction with IEC 60270, but these typically have an upper limit of 10 MHz. To measure at higher frequencies, the internal inductance must be reduced. This is achieved by reducing the capacitance of the coupler [22]. A proposed setup using capacitive PD coupling to measure at pulsed voltages is seen in Figure 7.

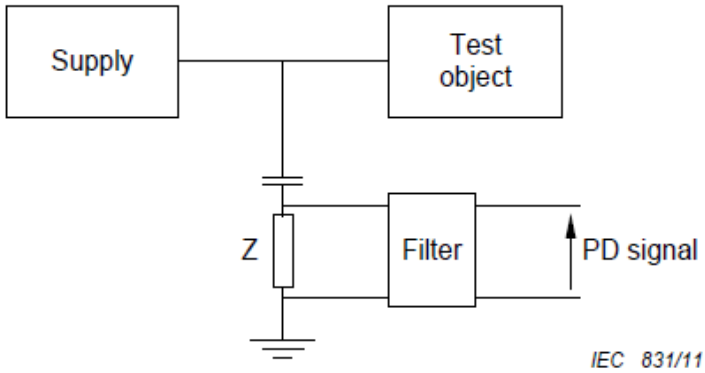

Figure 7 Capacitive coupling of PD signals, from [16].

2.1.3 Inductive PD coupler

Inductive PD couplers, also called L-sensors or HFCTs, are basically transformers where the conductor under examination acts as the primary coil with one "turn". As seen in the measurement circuit in Figure 8, the magnetic flux surrounding the primary conductor is captured by the secondary coil that is wound around a ferrite core with high permeability. When a current pulse $i_p(t)$ flows through the primary conductor, a voltage $v_p(t)$ is induced in the secondary coil [22].

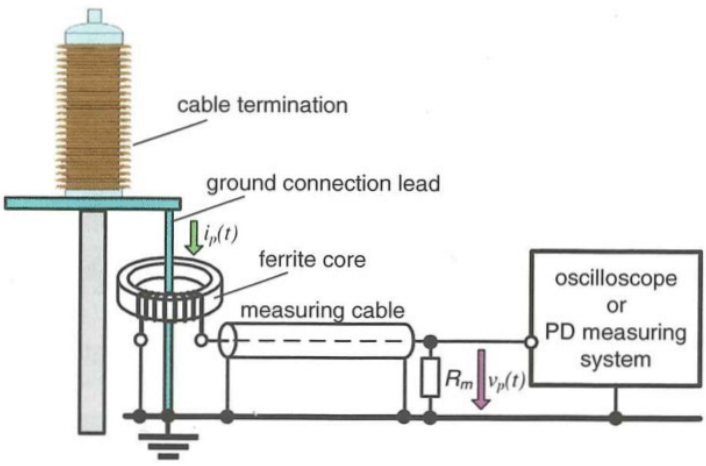

Figure 8 HF current probe measurement circuit, from [22].

2.2 Electromagnetic Measurements

Electromagnetic detection techniques are commonly used to detect PDs in the VHF and UHF range. An electromagnetic PD coupler operates similarly to an antenna in the near-field region [22]. During voltages with short rise times, monopole antennas have i.e. been used to detect PD in an inverter fed motor [23], and in a coil sample [20].

Detection of radiated electromagnetic signals can be done as seen in Figure 9. If an ultra-wideband (UWB) antenna is used, suppression of the applied voltage is needed. Suppression is not needed if the antenna has a cut-off frequency or narrow-band higher than the frequency content of the applied voltage [16].

The relationship between frequency (f), wavelength (λ) and speed of light (c) in air is given by Equation (1), and the relationship between antenna length (l) and wavelength for a straight wire monopole antenna is given by Equation (2).

$$\lambda = \frac{c}{f} \tag{1}$$

$$l = \frac{\lambda}{4} \tag{2}$$

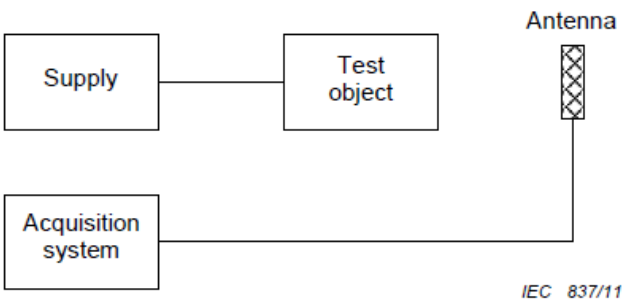

Figure 9 Electromagnetic PD detection using antenna, from [16].

2.3 Suppression of Applied Voltage

When measuring PD using either of the electrical detection methods or an UWB antenna, some form of suppression of the influence of the applied voltage is needed. This is because of the large currents induced in the test object during voltage commutation. Filtering the signal through a high-pass filter is suggested in the technical specification [16] and has earlier been used together with e.g. direct measurement [17], capacitive coupling [18, 19] and antenna [23]. Signal processing has also been proposed for suppressing the switching current pulse, using e.g. accumulated sum [18] or wavelet transform [21].

2.3.1 Filter

The frequency spectra of the applied voltage with short rise times and of the PD pulses typically overlap. An illustration of this overlap can be seen in Figure 10. To get a good signal to noise ratio when measuring PD, a high-pass filter can be used to suppress the frequencies of the voltage. The lower cut-off frequency of the high-pass filter to be used depends on the frequency spectrum of the applied voltage and should be selected as shown by the dotted line in Figure 10 [16].

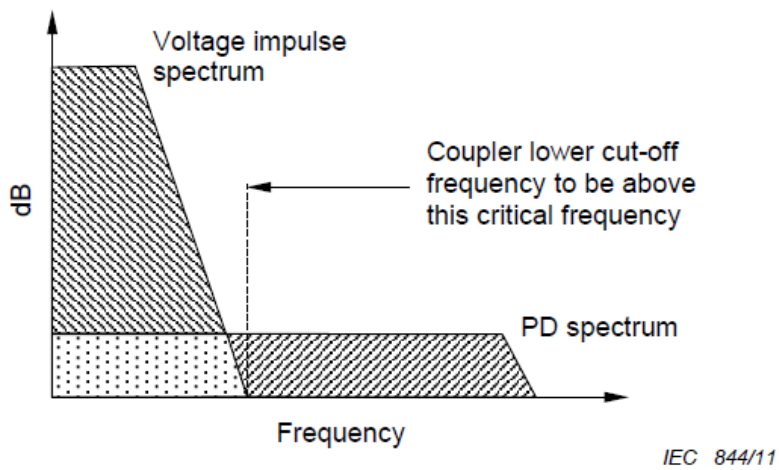

Figure 10 Overlap between voltage impulse and PD spectra, from [16].

2.3.2 Gating

Gating is suggested in the technical specification [16] as a different method of suppressing the switching current pulses. Gating can be used to block the signal flowing from the test object during the first part of the transient voltage. This means that the current pulse originating from the switching of the applied voltage is avoided. The problem with this method is that no real PDs will be detected in this region.

2.3.3 Signal Processing

Accumulated Sum

Lindell et al. [18, 24] has proposed a PD detection method where subtraction of accumulated sum is used for suppression of the influence of the applied voltage. Provided that the voltage source is stable and that every measurement starts at the same location on the phase, all measurements will have the same contribution from the applied voltage. PDs on the other hand are stochastic in nature and will happen at different phases with different amplitudes. This means that when subtracting the accumulated sum from a measurement containing PD, all you are left with is the PD pulse, as seen in Figure 11.

The accumulated sum (u_{acc}) is found using Equation (3) each time a signal (u_m) is recorded. m is the current iteration, and n is a constant that determines what impact the previous measured signal has on the sum.

$$u_{acc}(m) = \frac{u_m(\mathrm{m}) + n \cdot u_{acc}(\mathrm{m}-1)}{n+1} \tag{3}$$

One advantage of using this method rather than finding the mean value of the signal, is that only one measurement must be stored on the measurement system.

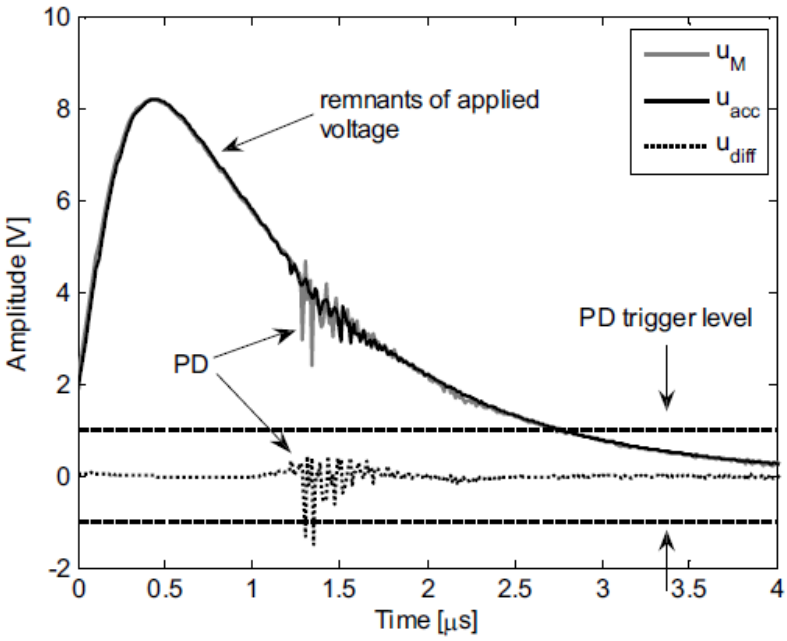

Figure 11 Using accumulating sum to suppress applied voltage contribution, from [24].

Wavelet Transform

Wavelet transform analyses a signal both in the frequency and time domain. A wavelet is a short signal with an average value of zero, and discrete wavelet transform DWT decomposes a signal into such wavelets. The signal is decomposed using a series of high-pass and low-pass filters together with down-sampling as seen in Figure 12 [25]. The high-frequency components of the signal are called details, and the low-frequency components is called approximations [25]. Each decomposition is called a "level". Choices that must be made when using DWT is; picking a mother wavelet, and number of levels to decompose the signal. To find a suitable mother wavelet, trial and error has been found to be the only option [25].

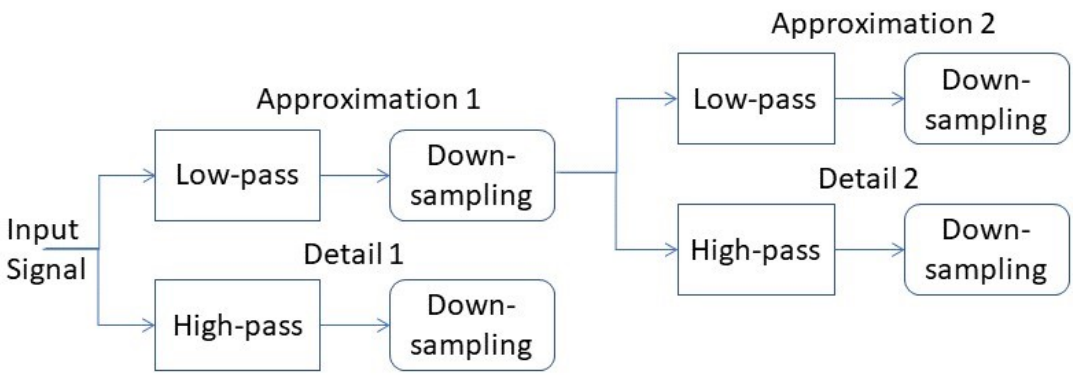

Figure 12 Wavelet decomposition, edited from [25].

Kjær et al. [21] has proposed a system where discrete wavelet transform (DWT) is used as a suppression technique together with a HFCT for measuring PD at transient voltages. Good results were achieved using the 8th order Daubechies mother wavelet (db8) at decomposition level 6 (d6). In Figure 13 seen from the top is; original signal, approximation (a8), details (d8-d1). At detail d6, a good signal to noise ratio is seen.

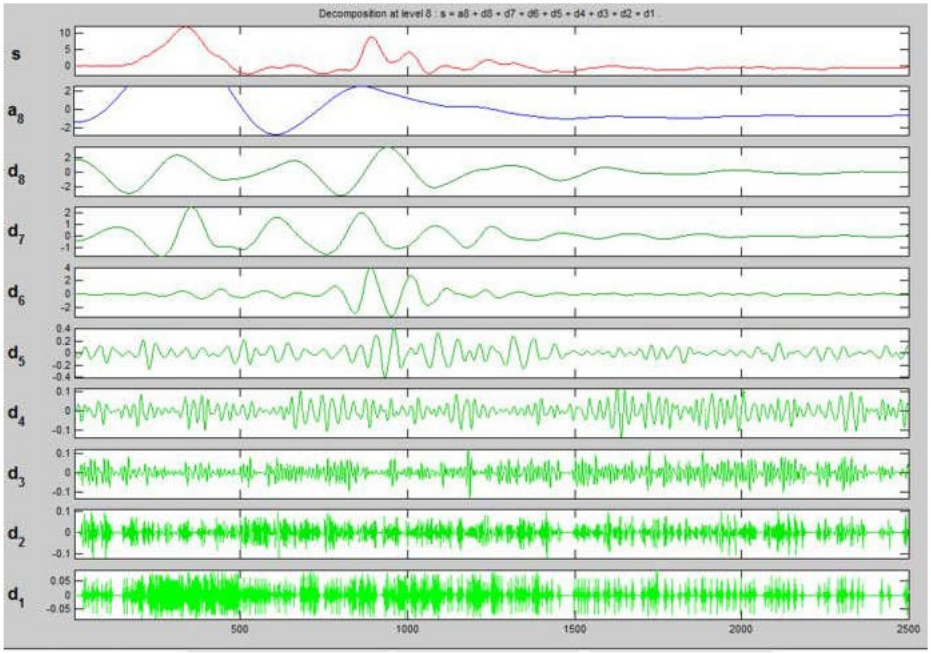

Figure 13 Level 8 decomposition using wavelet db8, from [21].

2.4 Optical and Acoustic Measurements

Optical PD detection has the advantage of being independent of the applied voltage and has earlier been applied successfully at voltages with short rise times [11, 20, 26], also on power electronic test objects [11, 26]. Light is emitted during PD activity, and instruments such as a photomultiplier (PM) can convert this light into electrical signals. A PM uses a process called photoemission to capture the light as electrons, these electrons are then multiplied to amplify the signal making the PM a very sensitive device [27].

PD also changes a materials local geometry causing energy to be released, a phenomenon called acoustic emission. Lundgaard has written an extensive article [28] on acoustic measurement of PD. Acoustic measurements are immune to electromagnetic noise, which is often a problem with electrical PD detection methods. In an earlier study [26] using a similar test setup, it was found that the charging and discharging of the test object created acoustic noise during the switching instants of the applied voltage. This made PD detection at the voltage flanks difficult, and acoustic detection has not been investigated further during this project.

3 EXPERIMENTAL METHOD

Two types of measurements have been performed in this project. A study in the frequency domain was done to characterize the applied voltage and PD pulses in the test object. PD measurements were done in the time domain, different techniques for measuring current and suppressing the influence of the applied voltage were investigated. The experimental setup consisted of the following elements which will be explained in detail later:

- Test object: Substrates for semiconductor converters encapsulated in silicone gel.
- Voltage source: High voltage (HV) pulse generator controlled from a LabVIEW program on a computer. The pulse generator with LabVIEW program was not made during this project and has been used in earlier similar projects.
- Voltage measurements: Tektronix HV probe with a 1000:1 ratio connected to an oscilloscope.
- Frequency measurement system: Spectrum analyzer - Hewlett Packard 8591E, 9 kHz – 1.8 GHz.
- PD measurement system:
    - Measuring interface: Different interfaces for measuring the current going through the test object.
    - Noise suppression: Different techniques for suppressing the current pulse resulting from the steep fronts of the applied voltage pulses.
    - Measuring device: Oscilloscope - Yokogawa DLM254, 2.5 GS/s, with USB connection and Matlab Tool Kit for connection with computer.
    - Control: Optical PD detection using a photomultiplier. This method was used earlier (Torkildsen [26]) on a similar setup and test object. It has now been used to check the electrical and electromagnetic measurements done here.

When performing measurements, the test objects, measuring interfaces and PM were placed in a lightproof cabinet to avoid disturbances during optical measurements. Pictures showing the experimental setup, and the inside of this cabinet with different measuring interfaces connected are shown in Appendix I.

3.1 Test Objects

In power electronic converters the semiconductors are soldered to a substrate, one of the most common substrate materials is aluminum nitride (AlN) [5]. Earlier studies [29] have shown that the electroluminescence of AlN substrates makes optical PD detection difficult. Because of this, printed circuit board (PCB) substrate models were used (Figure 14). The PCB substrates consists of an insulation layer with copper plates bonded to the top and bottom side. The overlap between the top and bottom copper plates is 8 mm, and the insulating layer is 1 mm thick. To simplify electrical connection, aluminum pins were soldered to the copper plates.

While most semiconductor substrates have two or more copper plates on the top side as seen in Figure 4, the test objects used in this project only has one. This was done for two reasons, minimizing risk of breakdown and conforming to testing practices. In an earlier study, Torkildsen [26] showed that there is a high risk of breakdown if measuring PD over the trench between two copper plates on the same side. To avoid damaging equipment due to a breakdown, measurements were instead performed over the insulating PCB layer. This also conforms to the way testing is performed today where the top side connections are short circuited.

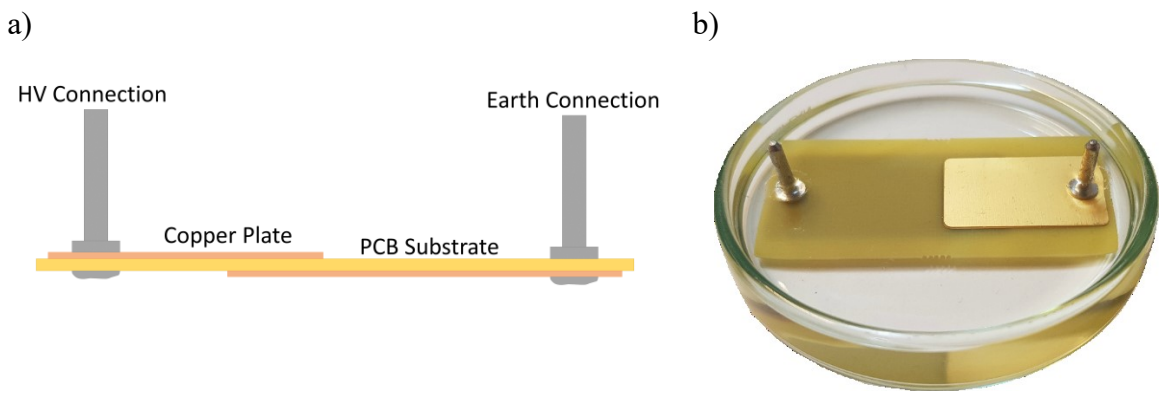

Figure 14 a Substrate sketch, **b** Substrate in a petri dish filled with silicone gel.

As mentioned earlier, silicone gel is the preferred material used to encapsulate power electronic modules. In this project, WACKER SilGel 612 A/B was used to encapsulate the substrates, as seen in Figure 14b. The gel is composed of two parts, A and B, which were mixed at a 1:1 ratio. To eliminate any air trapped in the gel or beneath the substrate, the test objects were placed in a vacuum chamber at 100-200 mbar for 30 minutes. The gel was then vulcanized by curing it in a heating cabinet at 100 °C for 15 minutes.

3.2 High Voltage Pulse Generator

The HV pulse generator (Figure 15) consists of two DC sources (V1A and V1B) charging two capacitor banks (C1A and C1B), and a fast bipolar transistor-switch between the capacitor banks and the output. The transistor switch has a maximum voltage of 65 kV per polarity, and a maximum peak current of 30 A. The current is in this project limited by two 1 kΩ resistances, R2 (A or B) and R3, which results in a maximum peak-to-peak voltage of 60 kV. The rise and fall times of the voltage is also determined by R2 and R3. R1A and R1B are large voltage dependent resistances (MΩ) responsible for limiting the current during charging of the capacitances.

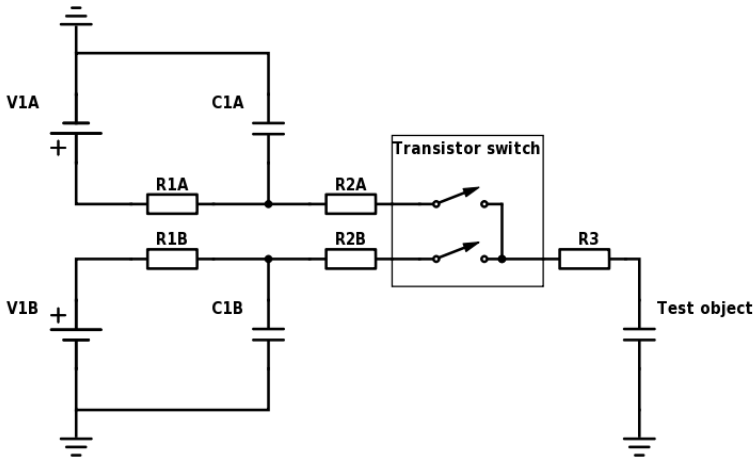

Figure 15 High voltage pulse generator.

The voltage levels of the dc sources are controlled from a LabView program on a computer. The frequency of the transistor switch is set by a signal generator which is also controlled from the computer. All measurements performed in this project were at a 50 Hz unipolar negative square wave, with a rise and fall time of approximately 300 ns.

The HV probe used for voltage measurements was not calibrated for the oscilloscope used, this caused the voltage shown on the scope to appear 10 % lower than it really was. All voltages referred to in this report are the actual voltages used.

3.3 Measuring Interfaces

Through examples from theory and guidance from supervisors, three different current measurement techniques were chosen: Direct measurement using a resistive shunt, inductive measurement using a HFCT and electromagnetic measurement using an antenna. All three interfaces were made during this project.

3.3.1 Resistive Shunt

A resistive shunt based on the principle shown in chapter 2.1.1 has been made, and a sketch drawn in AutoCAD when designing the shunt can be seen in Figure 16, the finished shunt is shown in Figure 17. The housing is based on a copper pipe with a copper lid on one side, and an isolating plastic lid on the other side. Instead of using a resistive cylinder, ten resistors were soldered to two circular copper plates at identical intervals to achieve a similar effect. Connection to the test object (top) and earth (top-right) is made with banana plugs, and the output is connected through a BNC plug. The ten parallel resistors are 1.2 Ω ± 5%, this results in the shunt having a resistance of 120 mΩ.

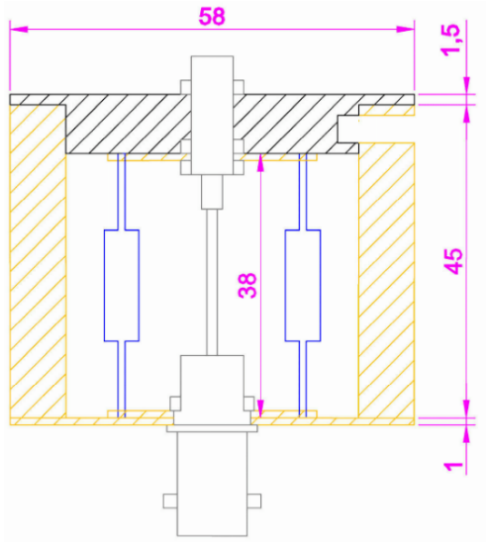

Figure 16 A sketch of the shunt made in AutoCAD. The shaded yellow areas are copper, the shaded black area is an isolating plastic and the blue areas are resistors. Connection to the test object (top) and earth (top-right) is made with banana plugs, and the output is connected through a BNC plug. Size annotations are in millimeters.

Figure 17 The finished resistive shunt.

3.3.2 High Frequency Current Transformer

A HFCT has been made following an example from Wyatt [30], see Figure 18. The probe is based around a clamp-on ferrite core from Würth Elektronik. A 1 mm^2 wire was wound seven times around one side of the ferrite core and glued in place. The wire was then connected to a BNC connector, one end to the center conductor and the other to the shield. Two rubber flanges were used to create a rigid structure.

It was attempted to identify the bandwidth of the HFCT. A 1 V signal with frequencies up to 50 MHz was measured using the HFCT. As seen in Figure 19, frequencies below 1 MHz are heavily damped, while a flat response is seen up to 50 MHz. Higher frequencies must be measured to find the full bandwidth of the device. Measurements performed by Wyatt [30] showed that this type of HFCT is comparable with a commercial HFCT up to a frequency of 600 MHz.

Figure 18 The finished high frequency current probe.

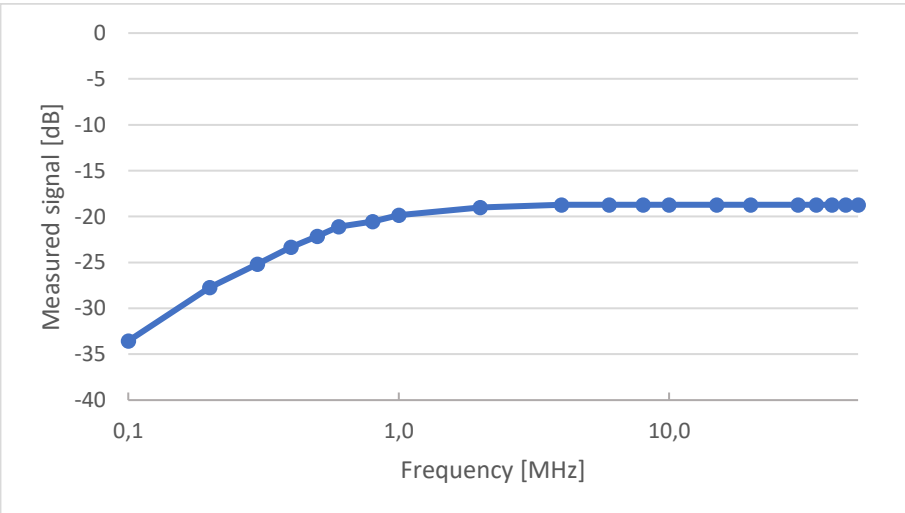

Figure 19 Measuring 1 V, 0.1 – 50 MHz test signal with the HFCT.

3.3.3 Antenna

A simple straight wire monopole antenna was made by extending the center conductor of a coax cable, see Figure 20. To make the antenna rigid it was fixed to an insulating structure. Through the frequency measurements that will be presented later it was found that the highest frequency content of the applied voltage was 300-500 MHz depending on the voltage level, while the PD had frequency content up to 1GHz.

The objective was to make an antenna with a center frequency of 600 MHz to get minimal damping of the PD signal and sufficient damping of frequencies pertaining to the applied voltage. Using the formulas in chapter 2.2, it was found that the antenna had to be 12.5 cm long to get a center frequency of 600 MHz.

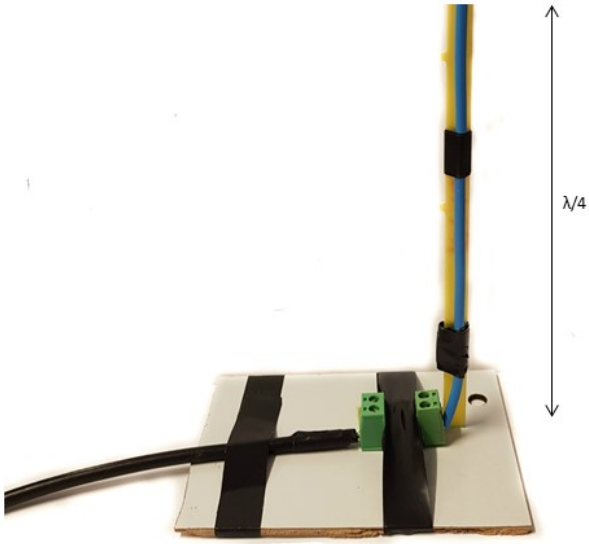

Figure 20 The finished straight wire monopole antenna.

3.4 Data Collection

Two Matlab programs were made for this project, one to control and receive data from the oscilloscope, and one to process the data. Yokogawa provides a MATLAB toolkit for the oscilloscope that includes functions specifically made for communication with the instrument.

A program called "ConnectAndRetrieve.m" based on an example in the tool kit manual [31], was made for collecting data from the measurements. The program has the following structure and functions:

- Open communication (1)
- Start signal acquisition (2)
- Transfer measured data to MATLAB matrix (3)
- Store matrix on computer as text file with custom name (4)
- Repeat step 2-4 until the wanted number of acquisitions are performed (5)
- Close communication (6)

When performing i.e. 20 acquisitions, the program will create 20 text files called "WaveData_*CustomText_Date_SequenceNumber*.txt". The text files contain the wave data for the chosen channels on the oscilloscope.

A second program, "ReadFiles.m", was made to read and process the text files made using "ConnectAndRetrieve.m". When starting the program, it will prompt the user to input the custom text and date of the files to be read. It will also prompt for sequence numbers, if a sequence of 20 measurements has been done, the user can choose to read one, a certain range or all of them. The wave data files are then read and combined into one matrix for each channel. Several optional ways to process the data has also been made:

1) Plotting the actual signal with or without the average voltage as a reference.
2) Plotting the signal compensated for average with or without the average voltage.
3) Electrical vs optical comparison.
4) Perform wavelet analysis and plot result.
5) Find PD pulses and plot scatter diagram.
6) Extra program to manually control each measurement

The complete Matlab programs with further explanations can be found in Appendix II.

3.5 Suppression of Applied Voltage

Three different techniques were chosen for suppressing the influence of the applied voltage: Filtering using a high-pass filter, and signal processing using wavelet analysis and subtraction by average.

3.5.1 High-Pass Filter

The only available and somewhat suitable high pass filter was a 200-1000 MHz pre-amplifier designed for a Power Diagnostix PD recording system (ICMsystem). The pre-amplifier is called RPA3 and can be seen in Figure 21. This is not a regular high-pass filter, but its functionality may still be suitable for this application. It takes the envelope of the 200-1000 MHz parts of the signal and transfers the envelope into a lower frequency range, 100-800 kHz. The output signal is also made unipolar positive and may be amplified using the ICMsystem.

Figure 21 Power Diagnostix RPA3 pre-amplifier 200-1000 MHz. The left BNC is connected to the test object via the measuring interface, the right is connected to the oscilloscope and the ICMsystem.

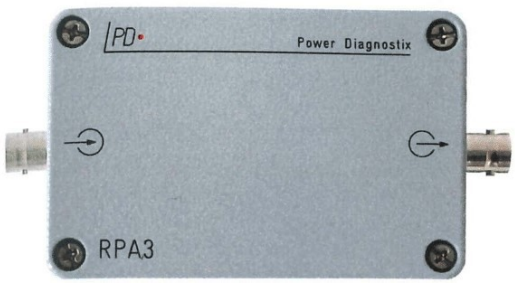

3.5.2 Signal Processing

Wavelet analysis and subtraction by average was implemented in the “ReadFiles” Matlab program.

- Wavelet: After trying different mother wavelets and decomposition levels, it was found that the 8th order Daubechies mother wavelet at decomposition level 7 gave the best results.
- Average: Subtraction by average was chosen instead of subtraction by accumulated sum that was presented in theory. This was because the processing of data was done post measurements, not simultaneously. The voltage waveform from all measurements are averaged, and this average was then subtracted from each of the measurements.

3.6 Noise in Experimental Setup

Two main sources of noise were found in the experimental setup, a high frequency noise from the pulse generator and dark pulses in the photomultiplier.

3.6.1 HV Pulse Generator

When connecting the "earth side" of the test object to the oscilloscope, repeating signal spikes were noticed even without the voltage source turned on. These spikes were significant in amplitude and had a repetition frequency of about 1.6 kHz. A lot of work was done to find the source of this noise.

After systematically disconnecting and connecting all possible sources in the test setup, it was believed that the noise originated from a box containing the transistor switch's power supply and TTL signal input. A picture of this box can be seen in Figure 22.

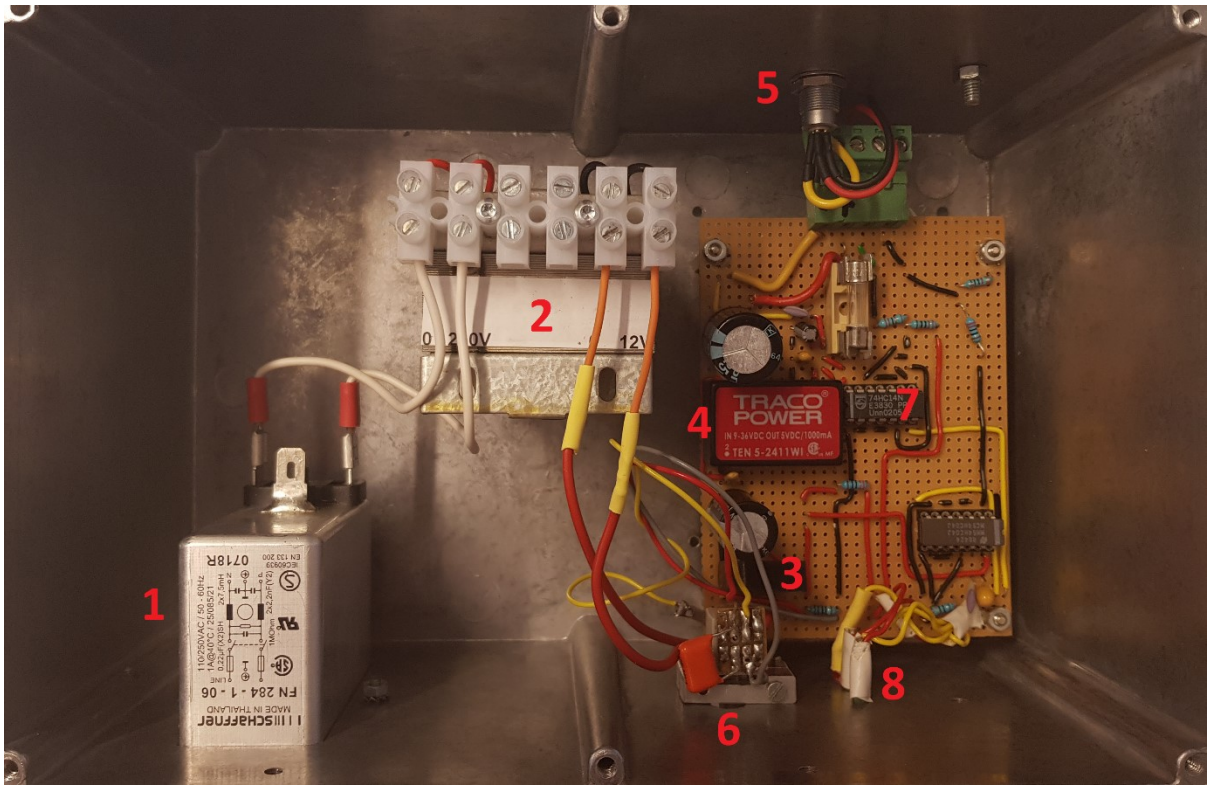

Figure 22 Power supply and TTL signal amplification for HV pulse generator. (1) Power entry module with filter and on/off switch. (2) 230 V to 12 V transformer. (3) Rectifier. (4) 12 VDC to 5 VDC converter. (5) Connection to transistor switch. (6) Fiber connection with TTL signal. (7) Circuit for TTL signal amplification and LED control (8) LEDs for power, operation and error.

The DC/DC converter was initially believed to be the cause of the noise as it utilizes pulse frequency modulation with a high switching frequency to step down the voltage. To check if this was the case the DC/DC converter was removed, and an analog DC power supply was integrated in the circuit to supply the 5 V. This did not remove the problem. To completely rule out the 5 V supply as the source, a 4,5 V battery from a portable USB charger was also mounted to the circuit board with no effect on the noise.

Another suspected cause was the part of the circuit responsible for receiving and amplifying the TTL signal. The TTL signal is supplied from a signal generator through a fiber connection, and then converted back to an electrical signal. This circuit is supplied by the same 5 V source, and to check if the TTL processing circuit was responsible for the noise, the wire supplying 5 V was removed to render the TTL part of the circuit without power. This did not solve the issue.

Some additional fixes were done without success, a missing earth connection was installed, a resistor with poor connection was improved and the output plug was replaced due to the possibility of interconnection of different signals.

The source of the noise signal was eventually found not to originate from this box at all. After discussing the problem with the manufacturer of the transistor switch, it was identified to be a “state refresh signal” originating from the switch itself. This signal is transmitted throughout both the HV and LV parts of the test setup and would be very difficult to remove. An option to temporarily pause the “state refresh signal” is available in newer versions of the transistor switch.

3.6.2 Photomultiplier

The photomultiplier will frequently emit small pulses even in a completely dark environment, in a pre-project Torkildsen [26] investigated these pulses. The amplitudes of the noise pulses are important to know, in order not to confuse them with pulses originating from PD activity. The noise pulses were recorded on the oscilloscope, and they behaved as illustrated in Figure 23. The amplitude ranged from 0 to 25 mV, and there was no correlation with voltage amplitude or phase time. The PD pulses registered during this project had an amplitude much higher than the amplitude of the noise pulses, and there was no problem distinguishing between the two.

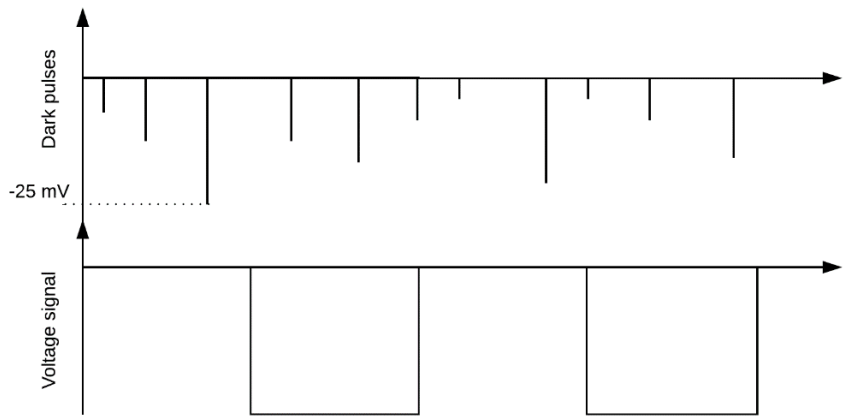

Figure 23 Illustration of recorded dark pulses.

3.7 Measurement Procedure

Two types of measurements have been performed in this project, frequency analysis of the switching and PD current pulses in the test object, and PD measurements using different techniques. The following subchapters explain how the measurements were performed.

3.7.1 Frequency Analysis

To measure the frequency characteristics of the signals going through the test object, the earth side of the test object was connected to a frequency analyzer, as seen in Figure 24. The rest of the equipment was used for gating purposes and will be explained later.

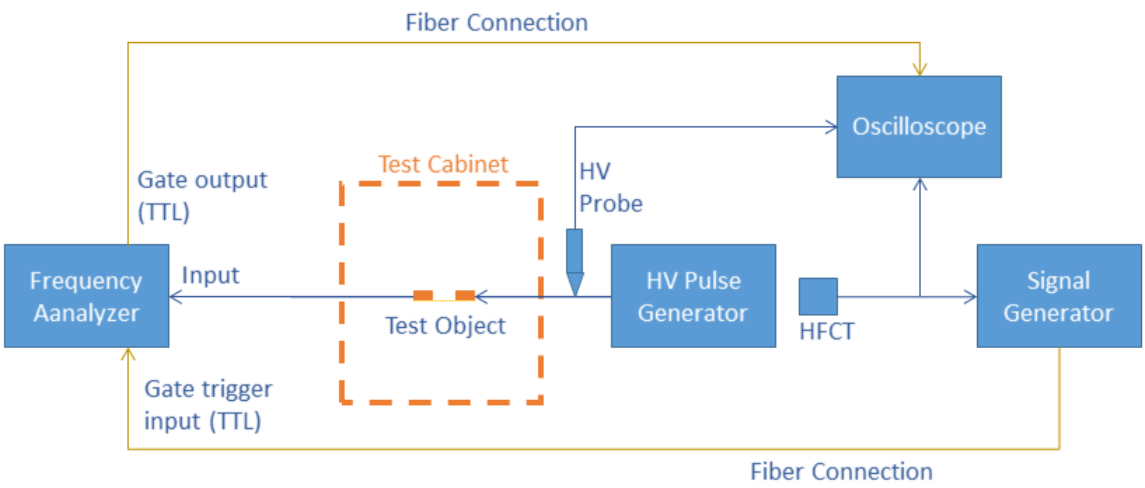

Figure 24 Test circuit during frequency measurements.

Gate Refresh Signal

As shown earlier, there was a noise signal originating from the HV pulse generator. The measuring circuit in Figure 24 was made to be able to gate away this noise signal when doing frequency analysis. A HFCT was clamped around a cable on the low voltage side of the pulse generator where the noise signal was strong, and it transmitted the noise signal to a signal generator. At the signal generator the noise signal was used to trigger a TTL signal. This TTL signal was sent to the frequency analyzer where it was used to synchronize a gate signal. By connecting the gate output signal from the frequency analyzer and the HFCT to the oscilloscope it was possible to fine-tune the gate around the noise signal as seen in Figure 25.

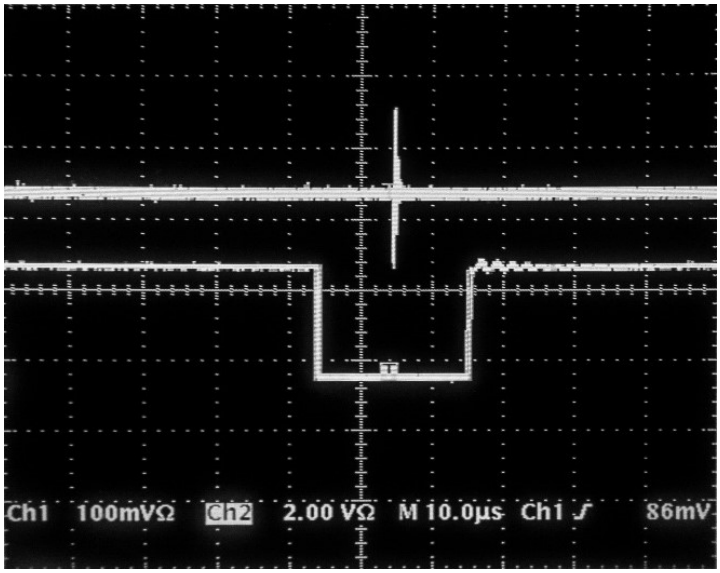

Figure 25 Gate refresh signal (top) and gating signal (bottom).

To find the effect of the gate refresh noise signal, the following measurements were done:

- Frequency spectrum with no voltage applied, but HV pulse generator turned on.
- Frequency spectrum with no voltage applied, but HV pulse generator turned on and gating applied.
- Frequency spectrum with a low voltage applied, with gating turned on.

Applied Voltage and PD Pulses

To find the frequency spectrum of the applied voltage and PDs in the test object, the frequency was analyzed at different voltage levels below and above PD inception voltage. A max-hold function was used, which means that the results show an envelope of the maximum amplitudes measured at each frequency.

The influence of the applied voltage and PD was compared in different ways:

- 2, 6 and 10 kV without PD.
- 6 kV without PD, 8 and 10 kV with PD.
- 10 kV with PD subtracted by 10 kV without PD.

3.7.2 PD Measurements

When doing PD measurements, the setup seen in Figure 26 was used. In addition to setting the applied voltage, the computer was used to start measurements and record waveform data from the oscilloscope. A HV voltage probe was used for voltage measurements. Different current measuring interfaces was connected between the test object and the oscilloscope. Optical measurements using a photomultiplier was done to check the electrical measurements.

All measurements were done at and around the flank of a 50 Hz unipolar negative voltage pulse, from 200 ns before the switching event until 1800 ns after. Measurements where performed here because this is where the measuring difficulties are. Additionally, the resolution would be poor if a long period is recorded.

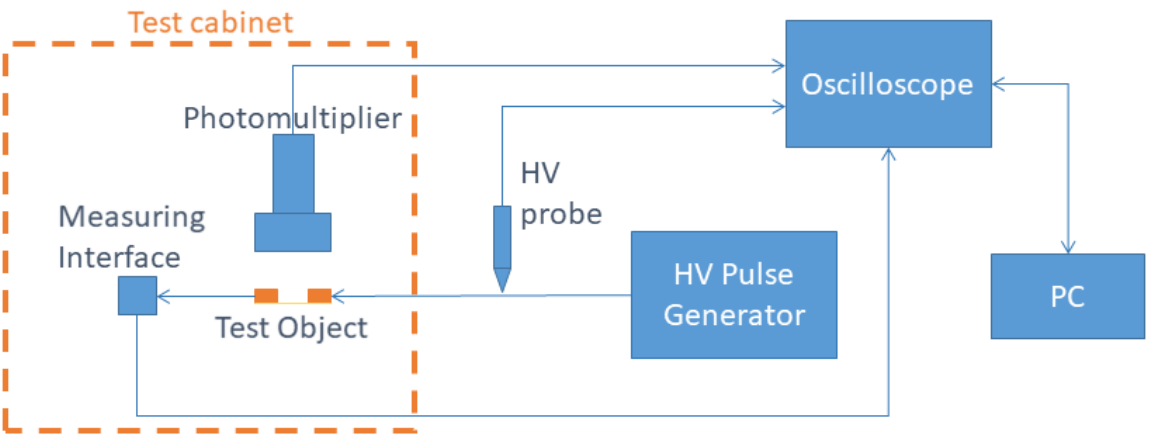

Figure 26 Test circuit during PD measurements.

Comparing Measuring Interfaces

The three measuring devices were all used to measure current through the test object at 14 kV. At this voltage level there was a sufficient amount of PD pulses, and PDs of equal size could easily be found. Measurements with PD pulses resulting in an equal response from the PM was chosen for comparison.

When measuring using the resistive shunt and HFCT, the current pulse due to the switching of the applied voltage was too high for the oscilloscope. Due to this, an attenuator was used to reduce the strength of the signal. The attenuator provided a damping of 10 dB in the range of DC up to 1 GHz.

Testing High-Pass Filter

To test the high-pass filter, the circuit seen in Figure 27 was used. The filter requires power from a Power Diagnostix ICMsystem to function, depending on the power it receives it can amplify the output signal. The ICMsystem was not used in any other way during testing of the filter, and the signal was transmitted to the oscilloscope for measuring using a coaxial t-coupler.

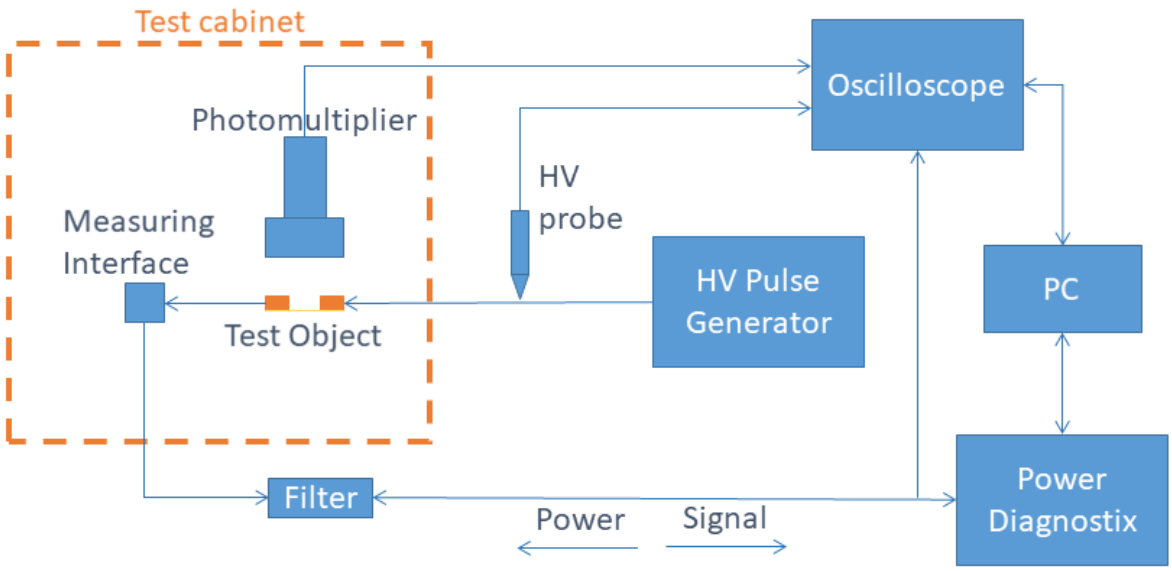

Figure 27 Measurement circuit using filter.

Testing the Signal Processing Techniques

To test the two signal processing techniques, a series of 20 measurements were recorded at 14 kV using the resistive shunt. The waveforms from these recordings were then processed using the appropriate options in the "ReadFiles" Matlab program.

Combining Methods to Create a Complete System

Combining the methods described earlier for current measurement, data collection and noise removal, a system for detecting PD pulses has been made. Resistive shunt is used for current measurement, Matlab is used for collecting measurement data, and correction for average is used to remove the switching current pulse.

A series of 100 measurements was done at the rising flank of both a 10 kV and a 16 kV applied voltage, and the falling flank of a 16 kV applied voltage. The wave-data from these measurements were collected using the "ConnectAndRetrieve.m" program and stored as separate text files on the computer. Using the option "Find PD pulses and plot scatter diagram" in the "ReadFiles.m" program, the data was processed.

The measurements were subtracted by average, and a search for peaks in the data were performed. To avoid noise being mistakenly registered as PD, only pulses with an amplitude above 100 mV was registered. To distinguish between oscillations and unique PD pulses, a delay of 100 ns between registering PD pulses was used. The amplitudes and positions of the PD pulses were then plotted in a scatter plot.

Additional Measurements

A comparison was done between PD amplitudes found using electrical and optical detection. This was done for 20 detected PDs at both the rising and the falling edge of a 16 kV applied voltage.

4 RESULTS AND DISCUSSION

A study in the frequency domain has been done to characterize the applied voltage and PD pulses. Different techniques for measuring current and suppressing the influence of the applied voltage were tested to create a system for PD detection. PD was then measured using this system. All measurements have been performed on the semiconductor substrate test objects at a 50 Hz square voltage with 300 ns rise time.

4.1 Frequency Analysis

Using a frequency analyzer, the test setup has been characterized during various conditions. Some initial measurements were done to find out how the gate-refresh noise signal originating from the transistor switch influences the frequency spectrum of the applied voltage.

In Figure 28, the following frequency spectra can be seen:

1) Gate-refresh noise signal, 0 V applied.
2) Gate-refresh noise signal, 0 V and gating applied.
3) 2 kV applied voltage with noise signal gated.

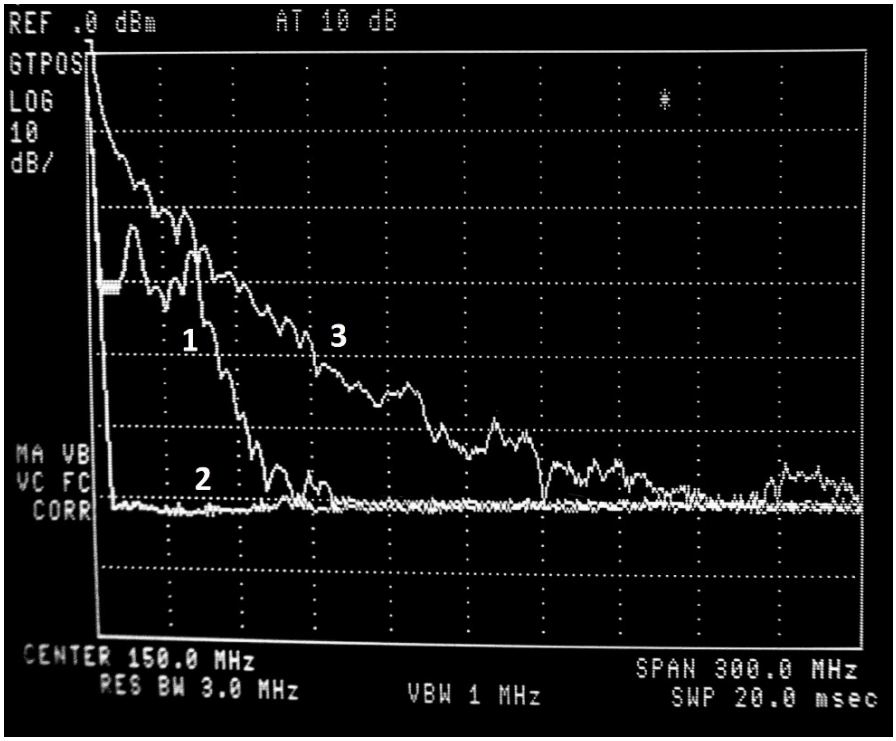

Figure 28 Frequency spectrum of noise signal (1), with gating applied (2), with 2 kV and gating applied (3).

It can be seen that the noise signal is successfully removed when applying the gate. It is also seen that the frequency spectrum of a small applied voltage is not affected by the noise pulses. This does not mean that the noise pulses do not pose a problem. The frequency spectra seen here are the maximum amplitudes measured at every frequency, and since the noise pulses are not synchronized with the applied voltage, they will appear both on the high-frequency flanks and the dc plateaus of the voltage. This may cause some uncertainties during PD measurements and will be discussed later. Newer versions of the transistor switch used in this setup have the possibility of pausing the gate-refresh signal during measurements, this would be preferred for future experiments.

The frequency spectrum of the current pulse caused by the voltage front has been found for voltage levels of 2, 6 and 10 kV. No PD was observed during these measurements. As seen in Figure 29, there were some changes in the frequency spectrum as the voltage increased. Most notably, the highest frequency content of the current pulse increased from ~300 MHz at 2 kV up to ~425 MHz at 10 kV. The amplitudes also increase, with the biggest differences found at higher frequencies. The reason for this voltage dependency of the frequency content is unclear but might result from small differences in the applied voltage shape or voltage dependent impedances somewhere in the measuring circuit.

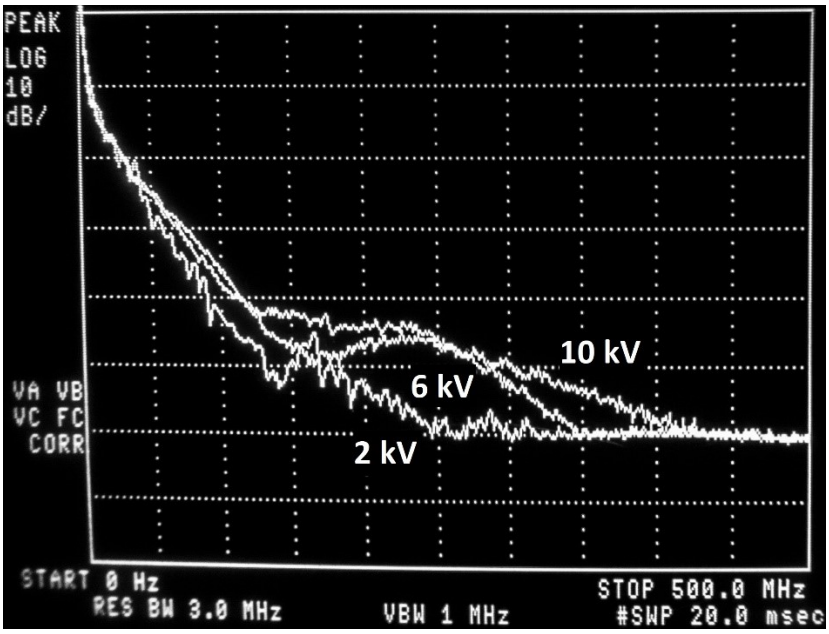

Figure 29 Frequency spectra of the applied voltage at 2, 6 and 10 kV.

The voltage was increased to a high level with a lot of PD activity and then reduced, this made it possible to observe PDs at voltage levels as low as 10 kV, which did not have PD during the previous measurements. A comparison has been done between the frequency spectra at 6, 10 and 14 kV, and as seen in Figure 30, the PD pulses have a large impact on both the amplitude and the bandwidth. At 6 kV there was no PD. At 10 kV the PD pulses has transformed the frequency spectrum. The amplitude has increased along almost the whole spectrum, and the highest frequency has increased from ~425 MHz to ~650 MHz. The amplitudes increase further at 14 kV while the highest frequency range stays the same. To extract the portion of the frequency spectrum originating from the PD pulses, a signal containing PD at 10 kV was subtracted by a 10 kV signal without PD, see Figure 31.

As mentioned earlier, the spectrums seen here are the envelopes of the highest amplitudes recorded at every frequency. This means that they strongly depend on the measurement time if the measured signal is irregular. The signals without PD is quite regular while the signals with PD is highly irregular because of the stochastic nature of PDs. No specific measurement times were used, the objective was to get an indication of the difference in frequency content between the current pulses originating from switching and from PD.

From the figures it is seen that at 10 kV a high-pass filter with 400 MHz cut-off frequency could be suitable for suppressing the current pulse caused by the voltage flank. A higher cut-off frequency is needed at higher voltages because of the increasing frequency content. Unfortunately, only a filter with 200 MHz cut-off frequency was tested during this project, and more suitable filters should be tested.

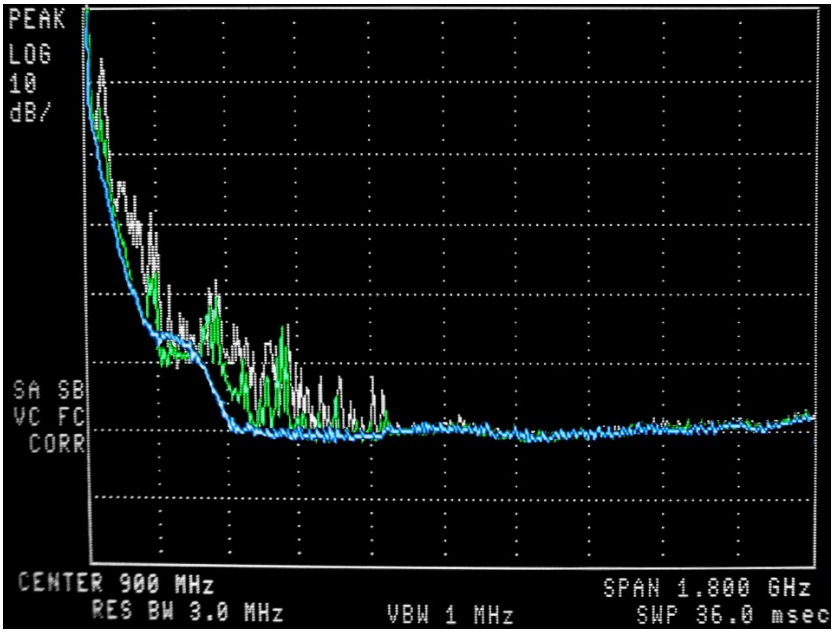

Figure 30 Frequency spectrum at 6 kV without PD (blue), 10 kV with PD (green) and 14 kV with PD (white).

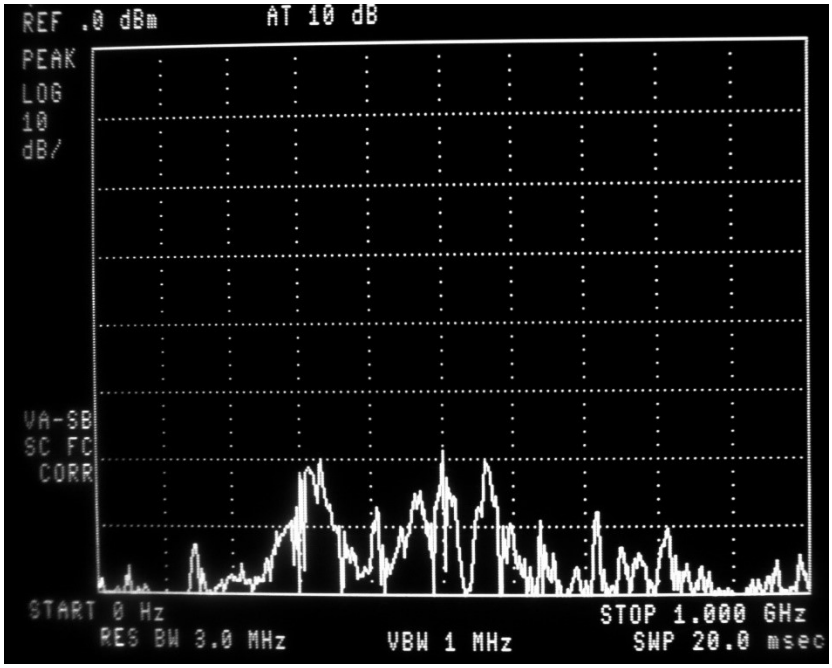

Figure 31 Frequency spectrum at 10 kV with PD subtracted by 10 kV without PD.

4.2 PD Detection System

Different techniques for measuring current and suppressing the influence of the applied voltage were tested to create a system for PD detection. PDs in substrate test objects were then measured using this system.

4.2.1 Current Measurement

To test the measuring interfaces, they were used to measure PD in the test objects at 14 kV. One PD pulse recorded using each of the three alternative measurement interfaces, resistive shunt, HF current transformer and antenna, is seen in Figure 32. 10 dB attenuation was used when measuring with resistive shunt and HFCT.

- Red waveform - signal from the interface.
- Purple waveform – signal from photomultiplier.
- Blue waveform – signal from HV probe.

The photomultiplier was used as verification that the pulses originates from PD events. As the three measurements were not done simultaneously, the PD pulses are not identical. PD events causing similar pulses from the photomultiplier (340-360 mV), were selected to make the three measurements as comparable as possible.

The three measuring interfaces provide quite different representations of the signal flowing through the test object. Both the pulse originating from the switching of the applied voltage and from PD can be seen clearly using all three. A comparison of some properties of the measured signal is seen in Table 1.

Table 1 Measuring interface comparison.

	Shunt	HFCT	Antenna
Switching pulse amplitude [V]	2,75	1,4	0,58
Switching pulse length [ns]	550	~1600	1400
PD pulse amplitude [mV]	200	150	200
PD pulse length [ns]	90	200	140

Using the resistive shunt results in the highest amplitude of the switching current, and the shortest settling time of the different interfaces. The HFCT will because of its nature, dampen the signal along its entire bandwidth, this results in a lower amplitude of the switching pulse than with the resistive shunt. It has the longest settling time of the three devices due to its high inductance. The antenna is narrowband, the exact bandwidth is unknown. The resulting damping of the switching pulse gives the lowest amplitude of the three interfaces, even when 10 dB attenuation was used with the other two. The antenna was designed to fit the frequencies of the PD pulses, and as intended, the PD pulse has not been damped as much. The antenna has a settling time between the other two interfaces.

The resistive shunt was chosen for use in the subsequent investigations. The high switching pulse will be suppressed, and a more important factor is the short settling time of the PD pulse.

a)

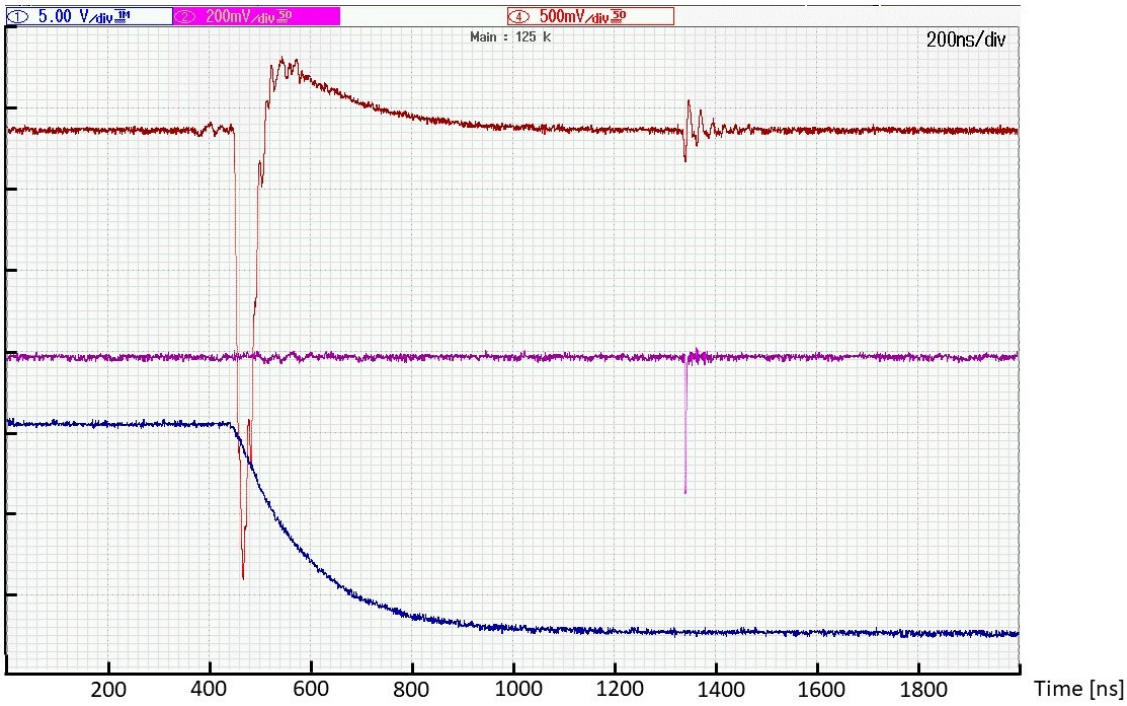

b)

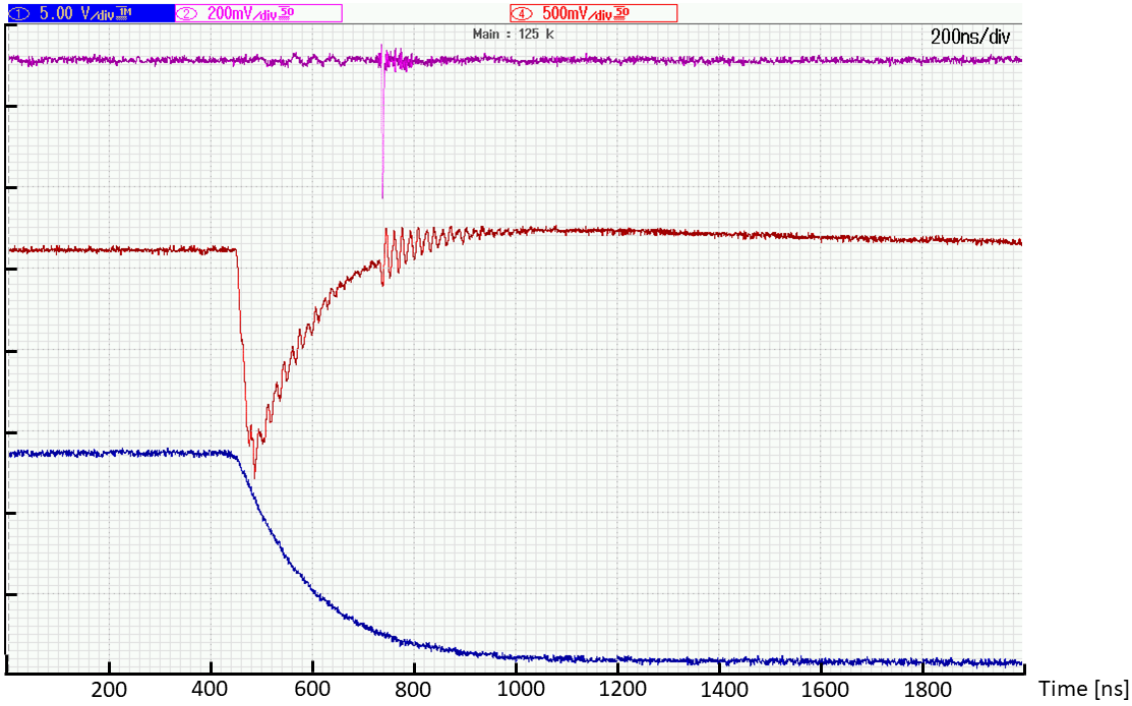

c)

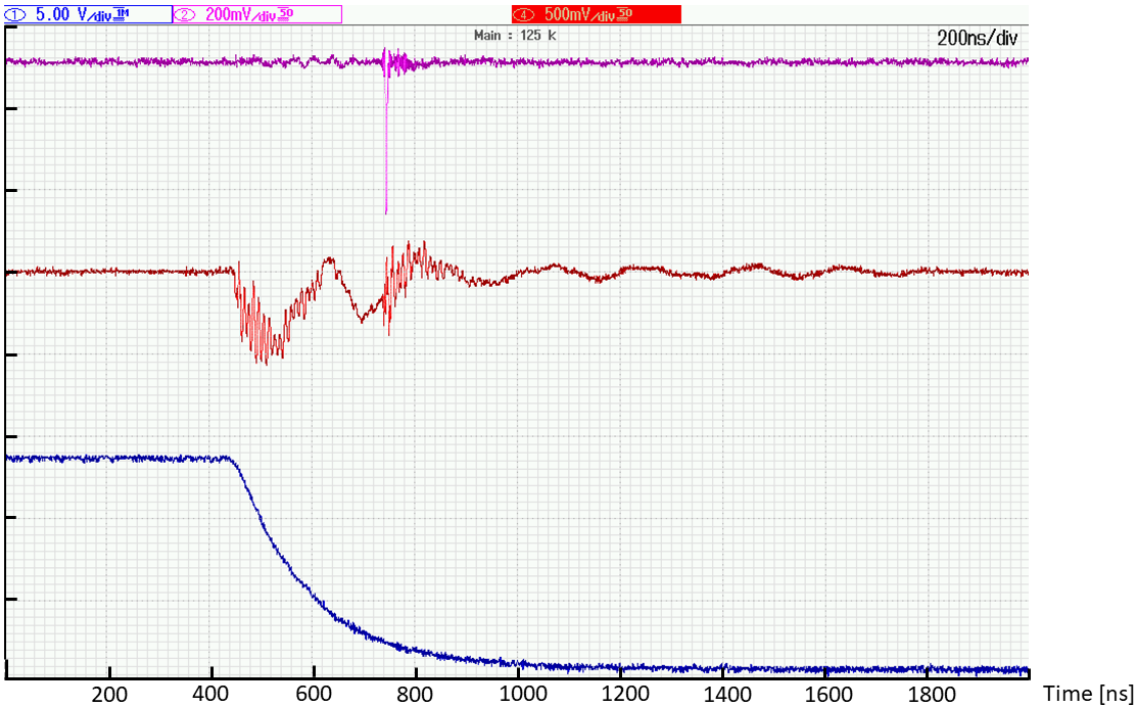

Figure 32 One PD pulse recorded using **a** resistive shunt (attenuated 10 dB), **b** HFCT (attenuated 10 dB), **c** antenna. Red waveform: signal from the interface, purple waveform: signal from photomultiplier, blue waveform: HV probe.

4.2.2 Data Collection

Using the Matlab program "ConnectAndRetrieve.m", wave-data can be recorded and made available for processing. As an example, 20 rising flanks of a 14 kV voltage has been measured and plotted together, see Figure 33. The plotting was done using the Matlab program "ReadFiles.m" option "Plot signal with/without averaged voltage". The average of the applied voltage from the 20 measurements has been included in the plot.

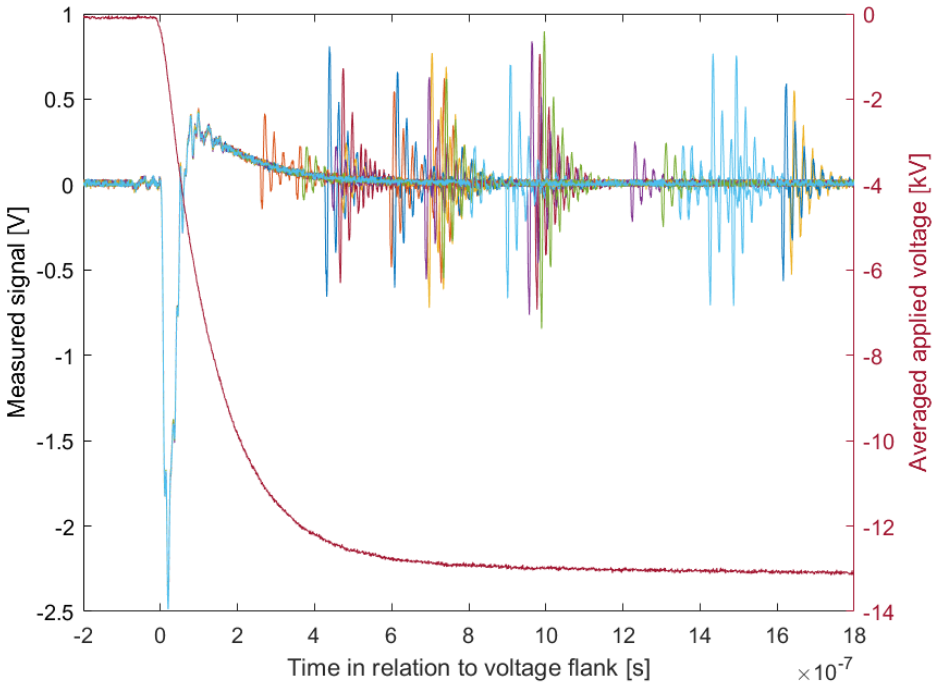

Figure 33 Actual measured signal at 20 rising voltage flanks.

The method used for data collection allows for easy post-processing of the data recorded. The time between measurements is about 5 seconds, this is too long and a big limitation of the data-collection system. Ideally, it should be possible to record consecutive voltage flanks. The data collection method used here does not allow for simultaneous PD detection, all processing must be done after the measurements.

4.2.3 Noise Removal

Different methods have been tested for suppression of the switching pulse to make it easy to find the number of PDs, their amplitude and position.

Filtering

A pre-amplifier has been used to remove the part of the current signal originating from the switching of the applied voltage. As we have seen earlier, the applied voltage has an upper frequency limit of 300-425 MHz (below PD inception levels). The pre-amplifier used has a frequency range of 200-1000 MHz and will only remove parts of the switching current pulse. As seen in Figure 34a, the switching current pulse has been reduced considerably and now is very similar to a PD pulse. It is also seen that the pre-amplifier has transformed the current pulse into a positive unipolar envelope of the original signal. This envelope has a ~20 ns delay compared to the optical and unfiltered PD pulse. Since parts of the applied voltage is let through the filter, there are problems detecting small PD pulses occurring during the voltage front. In Figure 34b, two small PD pulses can be seen, one of which is partly covered by the envelope of the switching pulse. Using the Matlab program, automatic detection of PD pulses is also made difficult by the remaining switching pulse as its size and shape is almost identical to that of a PD pulse.

A high-pass filter with cut-off frequency of 450 – 500 MHz would be better suited to suppress the switching pulses. Another alternative is to use the frequency analyzer as a narrow-band or zero-span filter at a frequency range containing PD exclusively.

a) b)

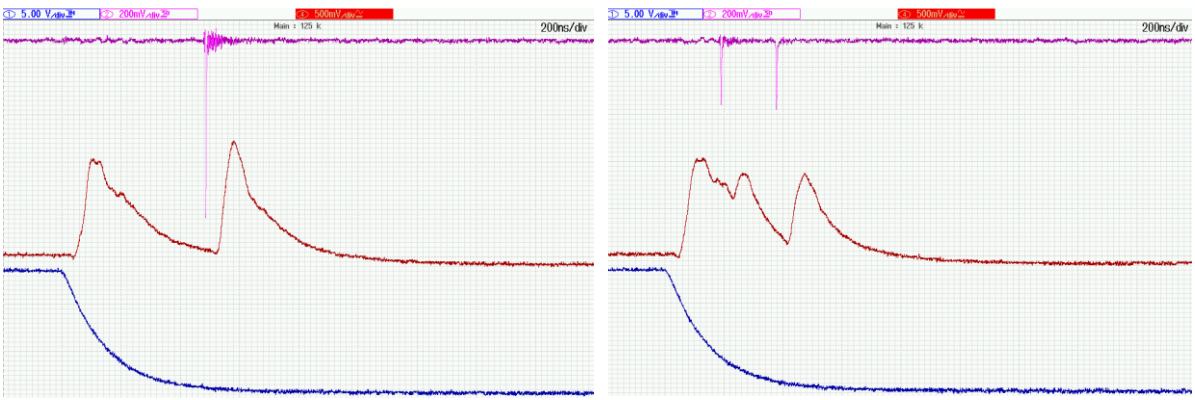

Figure 34 a One PD current pulse measured through 200-1000 MHz pre-amplifier. **b** Two PD pulses, one of which is partly covered by the switching current pulse.

Subtraction by Average

Another way of removing the switching pulse is through digital processing. One method used in this project is correction for average. By calculating the average of all current measurements, a waveform close to that of a current measurement without PDs is obtained. All the individual measurements are then subtracted by this averaged waveform to get a result as seen in Figure 35a. This processing and plot has been done using the Matlab program option "Plot current compensated for average with/without voltage". Just a few minimal noise spikes are left of the switching current pulse, and the PD pulses can easily be extracted for further processing. This is the same set of PDs seen unprocessed in Figure 33.

One problem with this method is that the averaged waveform will be affected by the PD pulses, this is more prominent if only a few measurements are done. In Figure 35b, the averaged waveform from measurements of 20 flanks (blue) and 100 flanks (orange) are compared. The average from 20 measurements is displaced by up to 72 mV which means that the amplitude of a PD pulse at this moment is reduced by 72 mV. The average from 100 measurements is displaced up to 30 mV.

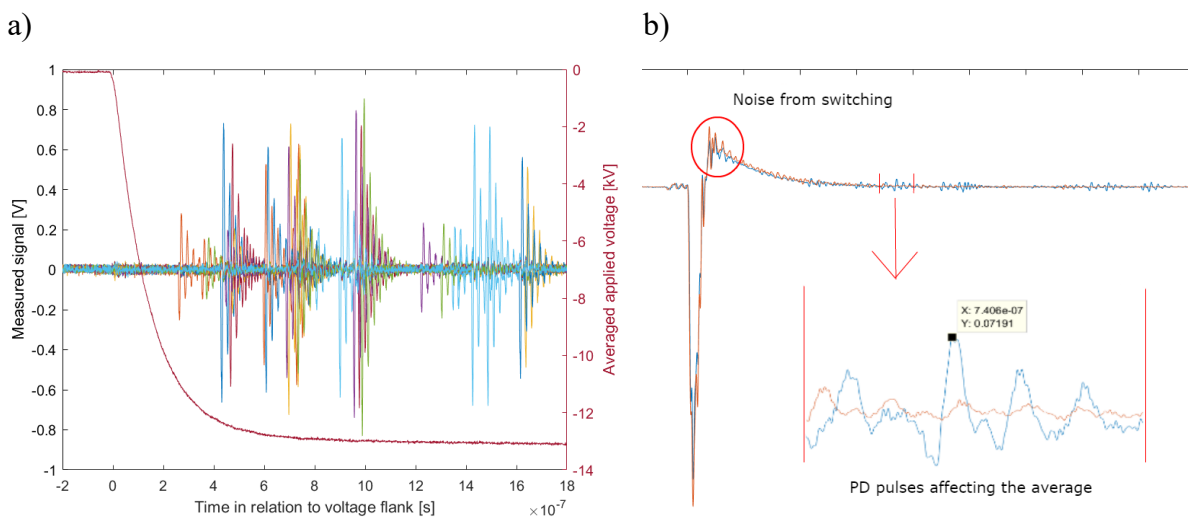

Figure 35 a Current measured during 20 voltage flanks corrected for average. **b** How the PD pulses affects the average at 20 (blue) and 100 (orange) measurements.

Wavelet Analysis

Wavelet analysis is another digital processing technique used in this project. As with filtering and subtraction of average, the objective was to remove the influence of the switching pulse current for easy extraction of data related to the PD pulses. Using the "ReadFile.m" Matlab program option "Plot wavelet analysis" a level 8 one-dimensional wavelet analysis was performed and plotted using the db8 wavelet.

A wavelet decomposition of a large PD pulse can be seen in Figure 36, the plot marked s is the original signal, a8 is the approximation coefficients and d7 shows the detail coefficients from level 7. The rest of the detailed coefficients (d1-d8) has been excluded from the figure. It can be seen that at level d7 the PD pulse has a high signal to noise ratio, and the switching pulse is removed. Using this, it is possible to extract data on the PD position and amplitude. But when doing the same analysis on a small PD pulse, Figure 37, it is seen that the signal to noise ratio is very low. Extracting information on this PD pulse would be impossible. A more suitable combination of wavelet type and detail level may exist, which would allow for this method to be used effectively.

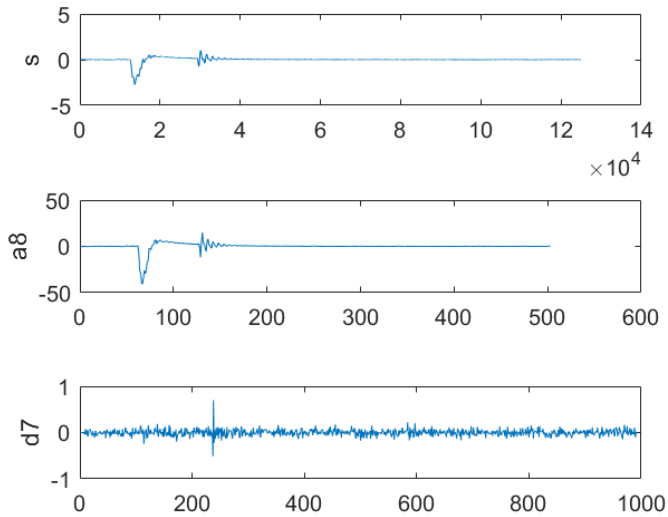

Figure 36 Wavelet analysis of large PD pulse.

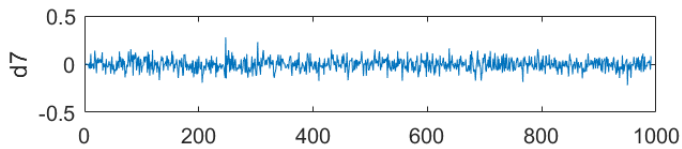

Figure 37 Wavelet analysis of small PD pulse.

4.2.4 Complete System

Combining the methods described earlier for current measurement, data collection and noise removal, a system for detecting PD pulses has been made. Resistive shunt is used as measuring interface, Matlab is used for collecting measurement data, and correction for average is used to remove the switching current pulse. A series of 100 measurements was done at the following voltage conditions:

- 10 kV rising flank
- 16 kV rising flank
- 16 kV falling flank

The data was then processed to find PD pulses. To avoid noise being mistakenly registered as PD, only pulses with an amplitude above 100 mV were registered. To distinguish between oscillations and unique PD pulses, a delay of 100 ns between registering PD pulses was used. The amplitudes and positions of the PD pulses were then plotted in a scatter plot as seen in Figure 38.

At 10 kV there was only three PDs registered, this implies that this voltage is close to the lowest voltage were PD occurs. The amplitude of the PDs registered at this voltage level is between 220 and 250 mV. At 16 kV on the other hand there were a lot more PD activity and the PD amplitudes ranged between 100 mV and 1.3 V, most between 300 mV and 1 V. There were approximately twice as many PDs at the rising flank of the voltage than at the falling flank. The amplitudes measured electrically were in the same range on both, this was not the case with the optically measured amplitudes as shown later.

No real PDs were registered before approximately 150 ns after the switching moment. This is halfway through the flank of the voltage. Most of the PDs occur during the rest of the flank or within 100 ns after. Further away from the flank a diminishing number of PDs are seen. The PDs of the two measurements at 16 kV form a prominent pattern. A “fan-shape” with a lot of PDs with rapidly increasing amplitude early, fewer PDs split into two different amplitude levels later. It is possible that if investigated more thoroughly in the future, the pattern of the PDs may provide information on what type of discharges are occurring in the test object.

A lot more measurements must be done to investigate PDs in these test objects properly. More measurements at the same voltage level to eliminate differences between test objects, different voltage levels, different rise times and different repetition frequencies should be investigated.

a)

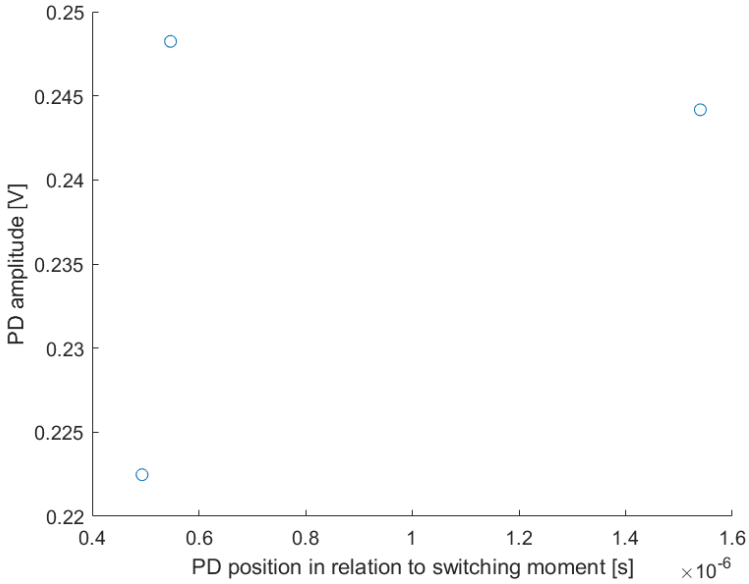

b)

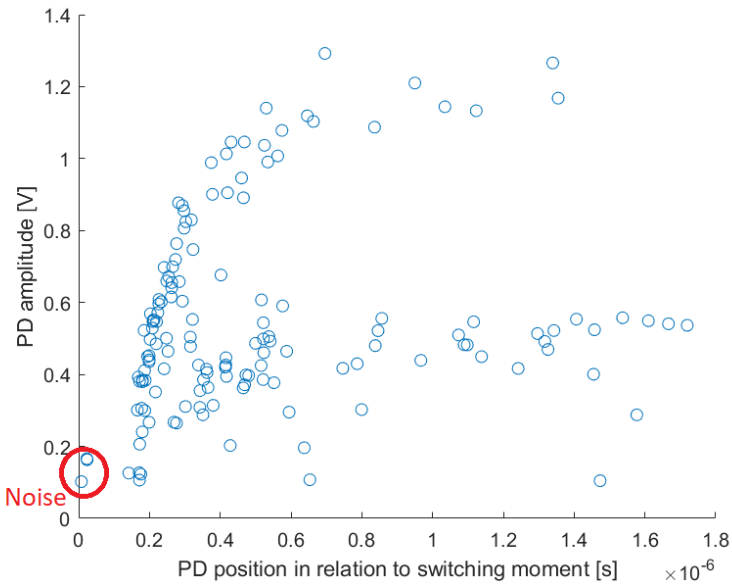

c)

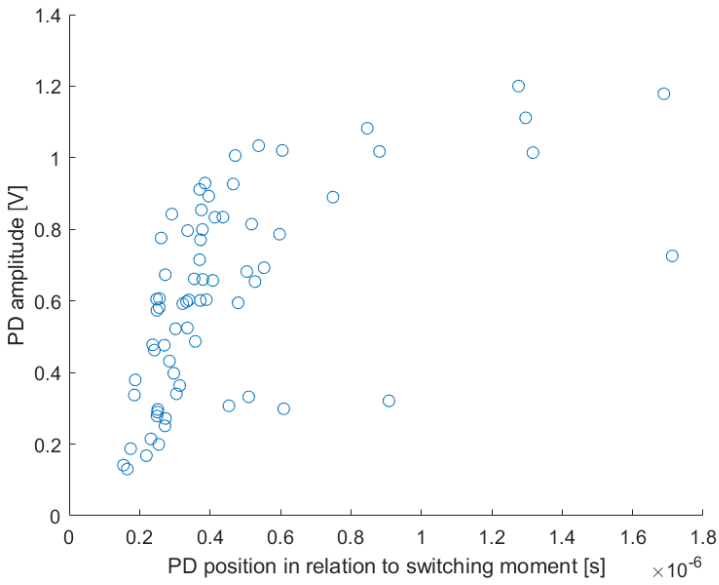

Figure 38 Detected PDs at 100 **a** 10 kV rising flanks **b** 16 kV rising flanks **c** 16 kV falling flanks.

A manual control of every measurement has been done. In Table 2, some key data describing the accuracy of the PD pulse classification can be seen.

Table 2 Accuracy data of the PD measurement system.

	10 kV Rising	16 kV Rising	16 kV Falling
Number of PDs detected	3	147	70
PDs not detected	0	11	0
- PDs below 100 mV	0	0	0
- PDs closer than 100 ns	0	11	0
PDs wrongfully detected	0	5	0
- Noise above 100 mV	0	4	0
- Oscillations longer than 100 ns	0	1	0
Largest amplitude detected	248 mV	1.29 V	1.20 V
Largest amplitude measured manually	267 mV	1.32 V	1.21 V

All PDs detected at the 10 kV rising flank and 16 kV falling flank were correct. Of the 147 PDs detected at 16 kV rising flank, five was not real PDs but noise reaching above the "detection limit" of 100 mV or PD oscillations longer than 100 ns. 11 PDs were not detected, this was all due to two or more pulses being closer than 100 ns as seen in Figure 39.

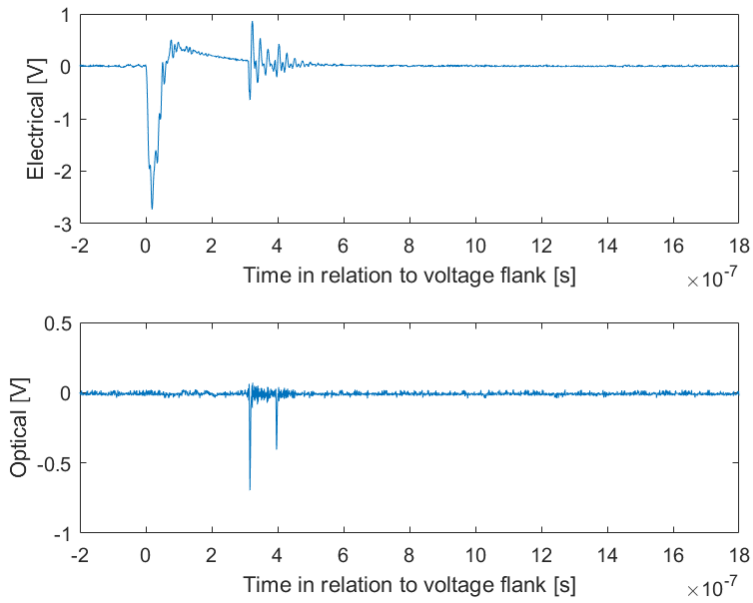

Figure 39 Two PD pulses very close together measured electrically (top) and optically (bottom).

Although this detection system has some faults, it will answer the most important question; are PDs occurring in the test object? Additionally, there may be somewhat easy corrections that can be made to avoid some of the measuring errors seen.

To detect PD pulses occurring closer together than 100 ns, a more advanced peak detection system can be implemented in the Matlab program. It must be able to differentiate between oscillations and a new PD pulse. This can be done by checking time and amplitude of every peak subsequent of the PD pulse. If a subsequent peak is found not to fit the trend of the oscillations, it will be classified as an individual PD pulse. This would also solve the problem of detecting oscillations longer than 100 ns as PD.

The automatically measured PD amplitude deviates with up to 30 mV compared to manually measured amplitude. This is a problem originating from the method of subtracting the average, and as discussed in chapter 4.2.3, the PD pulses affect the averaged waveform. This could be solved by implementing some additional smoothing of the averaged waveform in Matlab.

The noise pulses being detected as PD results from variations in the applied voltage during the switching pulse. The detection limit of 100 mV should not be raised, it should rather be lower in case of smaller PD pulses. The variation in the voltage may be a result of the state-refresh noise pulses presented in chapter 3.6.1, as these pulses had an amplitude of approximately 100 mV. If that is the case, an obvious solution is to upgrade the switch to a newer version which has the option to pause this signal. If the variations have another cause, this would be more difficult to solve. A possible solution is to apply a gate on the first 100 – 150 ns of the switching pulse. This is only applicable if no PD occurs during this time. No PDs were detected here in the measurements done in this project, but more measurements should be done to confirm this.

Voltages with different rise-times should be tested using this PD detection system. The measurements performed here were all at a square voltage with 300 ns rise time. In chapter 1.3 results from earlier research was presented claiming that shorter rise time may result in fewer PDs with higher magnitudes. This means that using this measurement system at a voltage with longer rise-times may be more difficult. More PDs could result in more difficulties separating individual PD pulses, and PDs with lower magnitudes could result in PDs and noise being harder to distinguish.

4.3 Additional Findings

A comparison has been done between the PD amplitudes registered on this PD detection system and optically on the PM. 20 consecutive PDs on both the rising and falling flank of a 16 kV voltage were compared, as seen in Figure 40.

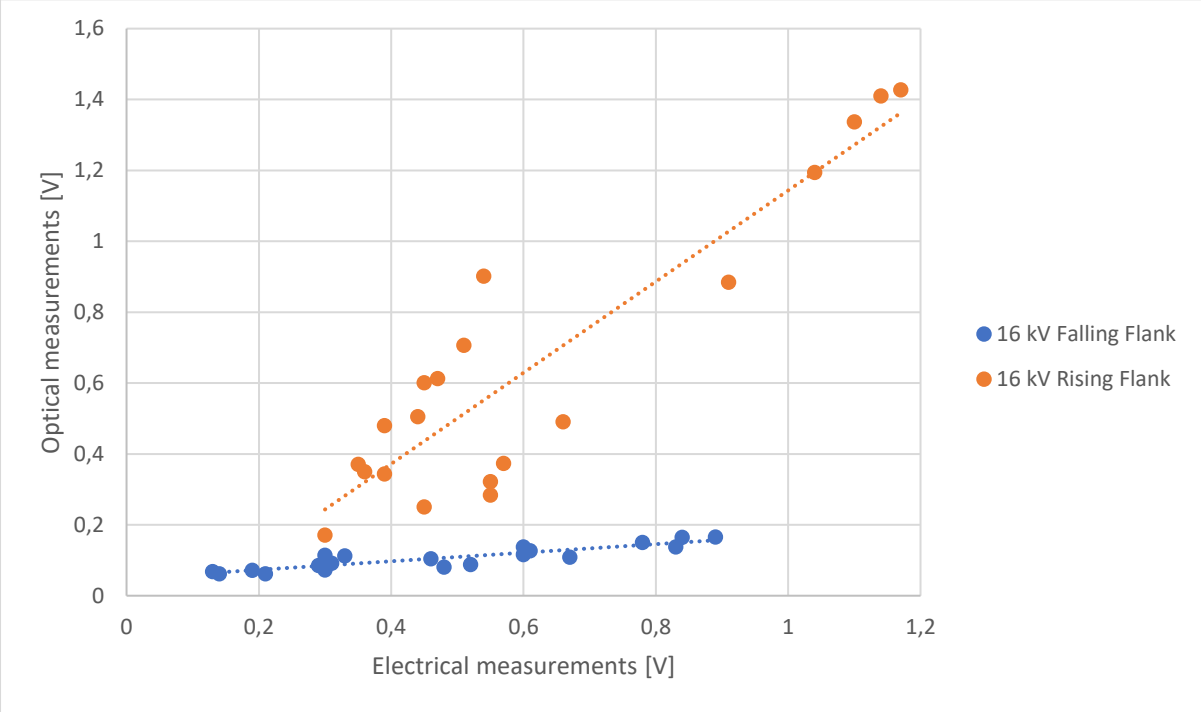

Figure 40 Electrical vs. optical PD amplitudes.

Even though there were some large deviations, the amplitudes found using the two techniques has a linear correlation. Of all the PDs detected here, or the 300 measurements in the previous subchapter, none were exclusively detected electrically or optically. This could indicate that that all PD activities on the substrate test objects are located in the silicone gel insulation, or that PD activity occurring inside the substrate is not detected using any of the methods.

The electrically detected amplitudes seen in Figure 40 are mostly in the same range on the rising and falling edge of the applied voltage. Contrary to this, there was a very large difference in optically detected PD amplitude between the rising and falling edge. As learned in chapter 1.3, the PDs on the falling flank is due to the building up of charge in the insulation material. Pulses with opposite polarity of the applied voltage will then occur. This does not explain the difference in optically detected amplitude, and an explanation for this has not been found. The results presented here does however indicate that electrical detection is better suited for PD detection at the falling flank of a pulsed voltage.

5 CONCLUSION

A system for PD detection during a fast-rising square voltage has been made. This system has then been used to detect PD in semiconductor substrate test objects.

The influence of the applied voltage and PD pulses on the frequency content of the current through the test object has been found using a frequency analyzer. The current pulse due to the applied voltage was found to contain frequencies up to 425 MHz at 10 kV and increasing with the voltage. PD pulses was shown to contain frequencies up to 1 GHz.

Three different interfaces for measuring the current through the test object have been made for direct, inductive and electromagnetic measurements respectively; resistive shunt, HFCT and antenna. A comparison done between the three methods showed the following: The resistive shunt had the lowest suppression of the current pulse caused by the switching of the applied voltage. The resistive shunt also had the shortest settling time of both the switching pulse and the PD pulse, the HFCT had the longest settling time. The PD pulse measured using the antenna was the hardest to separate from the surrounding noise.

Three different methods of suppressing the influence of the applied voltage has also been tested; filter, wavelet analysis and subtraction by average. The filter had a bandwidth of 200 – 1000 MHz and did not suppress the switching pulse sufficiently. As shown in the frequency analysis, a 450 – 500 MHz high-pass filter would be more suitable. The wavelet analysis done was able to get a good signal to noise ratio with a large PD pulse, but not with a small PD. The best suppression of the switching current pulse was achieved when using suppression by average.

Combining the best method for measuring the current and noise suppression, a functioning PD measuring system has been made. A standard oscilloscope connected to a computer with Matlab was used for data collection. Current measurements were done using the resistive shunt. A Matlab script was made to suppress the influence of the applied voltage using the subtraction by average method. This script was also used to plot the amplitude and location of the detected PD pulses.

The measuring system was able to detect PD both at low voltages with very little PD activity, and at higher voltages with a lot of PD activity. Some measuring errors are seen when the PD pulses occur at rapid succession and due to variation in the applied voltage.

More measurements must be done to verify the functionality of the measuring system and to properly investigate PDs in semiconductor substrates. One interesting finding in the experiments performed here, is that electrical PD detection seems to be preferable for more accurate measurements of PD amplitudes at the falling flank of a pulsed voltage.

5.1 Suggestions for Further Work

- An updated version of the transistor switch used in the HV pulse generator should be used. In the new version it is possible to pause the "state-refresh signal" creating noise in this setup.
- Measurements should be performed using a more suitable filter for noise suppression. Two alternatives are:
    - High-pass filter with cut-off frequency of 450 – 500 MHz.
    - Frequency analyzer used as a narrow-band or zero-span filter at frequencies above the highest frequency content of the applied voltage.
- More measurements must be done at voltages with different properties to confirm the functionality of the detection system presented here. Some changes should be done to the data processing system to avoid some of the measuring errors seen.
- The implementation of some form of commercially available PD detection system (e.g. ICMsystem from Power Diagnostix) should be investigated, as the system used here is only suitable for experimental purposes.
- More measurements at voltages with different properties such as rise-time, pulse length and repetition rate must be done to properly investigate PD in semiconductor substrates.

6 BIBLIOGRAPHY

[1] REN21, "Renewables 2017 - Global Status Report," Ren21, Paris, France2017.

[2] T. Bengtsson *et al.*, "Repetitive fast voltage stresses - Causes and effects," *IEEE Electrical Insulation Magazine,* Article vol. 25, no. 4, pp. 26-39, 2009.

[3] C. Buttay, "PWM principle," Pwm.png, Ed., ed, 2006.

[4] C. W. G. D1.43, "Insulation Degeneration Under Fast, Repetitive Voltage Pulses," ed: Cigré, 2017.

[5] A. Volke and M. Hornkamp, *IGBT Modules, Technologies, Driver and Application*, Second ed. Munich, Germany: Infineon Technologies AG, 2012.

[6] T. M. Do, O. Lesaint, and J. L. Augé, "Streamers and partial discharge mechanisms in silicone gel under impulse and AC voltages," *IEEE Transactions on Dielectrics and Electrical Insulation,* Article vol. 15, no. 6, pp. 1526-1534, 2008, Art. no. 4712654.

[7] P. Romano *et al.*, "Partial discharges on IGBT modules: Are sinusoidal waveforms sufficient to evaluate behavior?," in *2014 IEEE Conference on Electrical Insulation and Dielectric Phenomena, CEIDP 2014*, 2014, pp. 224-227.

[8] B. Florkowska, J. Roehrich, P. Zydroń, and M. Florkowski, "Measurement and analysis of surface partial discharges at semi-square voltage waveforms," *IEEE Transactions on Dielectrics and Electrical Insulation,* Article vol. 18, no. 4, pp. 990-996, 2011, Art. no. 5976086.

[9] A. Madonia, P. Romano, T. Hammarström, S. M. Gubanski, F. Viola, and A. Imburgia, "PD characteristics at square shaped voltages applying two different detecting techniques," in *Annual Report - Conference on Electrical Insulation and Dielectric Phenomena, CEIDP*, 2016, vol. 2016-December, pp. 247-250.

[10] P. Wang, A. Cavallini, and G. C. Montanari, "The influence of square voltage rise time on partial discharge spectra," in *Annual Report - Conference on Electrical Insulation and Dielectric Phenomena, CEIDP*, 2012, pp. 129-132.

[11] A. A. Abdelmalik, A. Nysveen, and L. Lundgaard, "Influence of fast rise voltage and pressure on partial discharges in liquid embedded power electronics," *IEEE Transactions on Dielectrics and Electrical Insulation,* vol. 22, no. 5, pp. 2770-2779, 2015.

[12] T. Shimazaki, "Flashover characteristics and surface processes under negative impulse voltage in atmospheric air," *IEEE Transactions on Electrical Insulation,* vol. 27, no. 3, pp. 488-495, 1992.

[13] Q. Liu and Z. D. Wang, "Secondary reverse streamer observed in an ester insulating liquid under negative impulse voltage," *Journal of Physics D: Applied Physics,* Article vol. 44, no. 40, 2011, Art. no. 405203.

[14] D. Frey, J. L. Schanen, J. L. Auge, and O. Lesaint, "Electric field investigation in high voltage power modules using finite element simulations and partial discharge measurements," in *38th IAS Annual Meeting on Conference Record of the Industry Applications Conference, 2003.*, 2003, vol. 2, pp. 1000-1005 vol.2.

[15] F. Breit, E. Dutarde, J. Saiz, T. Lebey, D. Malec, and S. Dinculescu, "Partial discharge detection in power modules," in *2002 IEEE 33rd Annual IEEE Power Electronics Specialists Conference. Proceedings (Cat. No.02CH37289)*, 2002, vol. 2, pp. 748-752 vol.2.

[16] *IEC/TS 61934, Electrical measurement of partial discharges (PD) under short rise time and repetitive voltage impulses*, 2011.

[17] D. Fabiani, G. C. Montanari, A. Cavallini, and G. Mazzanti, "Relation between space charge accumulation and partial discharge activity in enameled wires under PWM-like voltage waveforms," *IEEE Transactions on Dielectrics and Electrical Insulation,* vol. 11, no. 3, pp. 393-405, 2004.

[18] E. Lindell, T. Bengtsson, J. Blennow, and S. M. Gubanski, "Measurement of partial discharges at rapidly changing voltages," *IEEE Transactions on Dielectrics and Electrical Insulation,* Conference Paper vol. 15, no. 3, pp. 823-831, 2008, Art. no. 4543120.

[19] F. Guastavino, A. Dardano, and E. Torello, "Measuring partial discharges under pulsed voltage conditions," *IEEE Transactions on Dielectrics and Electrical Insulation,* Article vol. 15, no. 6, pp. 1640-1648, 2008, Art. no. 4712668.

[20] H. Naoki, I. Hiroshi, and O. Hitoshi, "Partial discharge inception characteristics by different measuring methods in magnet wire under surge voltage application," in *2007 Annual Report - Conference on Electrical Insulation and Dielectric Phenomena*, 2007, pp. 128-131.

[21] S. V. Kjær and J. Holboell, "System for detection and analysis of partial discharges under transient voltage application," in *Proceedings of the Nordic Insulation Symposium*, 2013, no. 23.

[22] W. Hauschild and E. Lemke, *High-Voltage Test and Measuring Teqhniques*. Berlin Heidelberg: Springer, 2014.

[23] D. Fabiani, A. Cavallini, and G. C. Montanari, "A UHF Technique for Advanced PD Measurements on Inverter-Fed Motors," *IEEE Transactions on Power Electronics,* vol. 23, no. 5, pp. 2546-2556, 2008.

[24] E. Lindell, T. Bengtsson, J. Blennow, and S. M. Gubanski, "Evaluation of a PD measuring system for repetitive steep voltage waveforms," *IEEE Transactions on Dielectrics and Electrical Insulation,* Article vol. 18, no. 1, pp. 246-255, 2011, Art. no. 5704516.

[25] G. Suganya, S. Jayalalitha, K. Kannan, and S. Venkatesh, "Survey of de-noising techniques for partial discharge interferences," *ARPN Journal of Engineering and Applied Sciences,* Article vol. 12, no. 2, pp. 414-427, 2017.

[26] M. L. Torkildsen, "Experimental Study of Power Electronic Substrates Exposed to Pulse Voltage Waveforms," Specialization Project, 2017.

[27] RCA, *Photomultiplier Manual - Theory, Design, Application*. Harrison, New Jersey, USA: RCA Corporation, 1970.

[28] L. E. Lundgaard, "Partial Discharge - Part XIV: Acoustic Partial Discharge Detection - Practical Application," *IEEE Electrical Insulation Magazine,* Article vol. 8, no. 5, pp. 34-43, 1992.

[29] J. L. Augé, O. Lesaint, and A. T. Vu Thi, "Partial discharges in ceramic substrates embedded in liquids and gels," *IEEE Transactions on Dielectrics and Electrical Insulation,* Article vol. 20, no. 1, pp. 262-274, 2013, Art. no. 6451366.

[30] K. Wyatt, "The HF Current Probe: Theory and Application," *Interfernce Technology,* 2012.

[31] Yokogawa, "Sample Program 2 from MATLAB Tool Kit User's Manual," vol. 11, ed: Yokogawa, 2017.

7 APPENDICES

7.1 Appendix I – Pictures of Experimental Setup

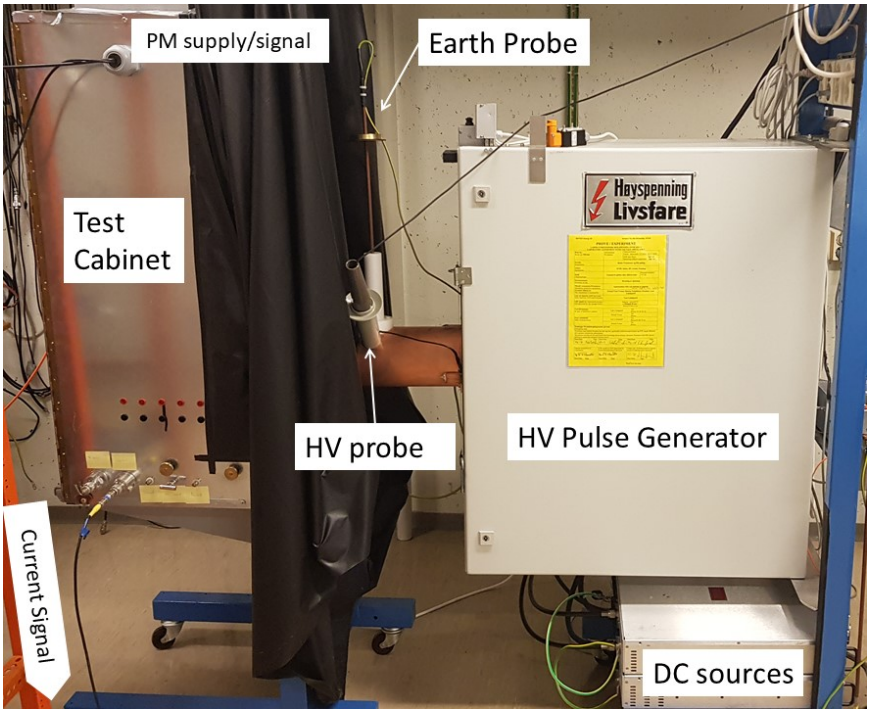

Figure 41 Picture showing the cabinets containing the pulse generator and measuring equipment.

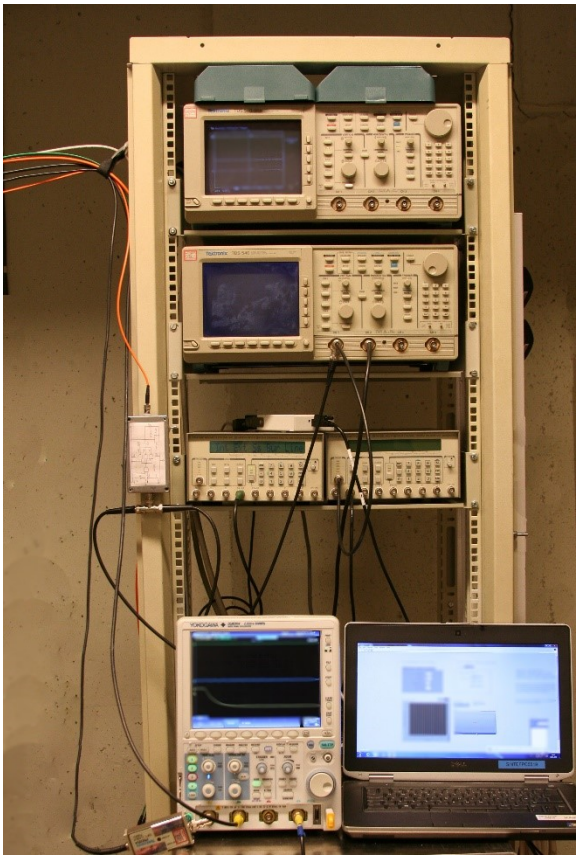

Figure 42 Some of the measuring equipment used, together with the PC used to control applied voltage and collect data.

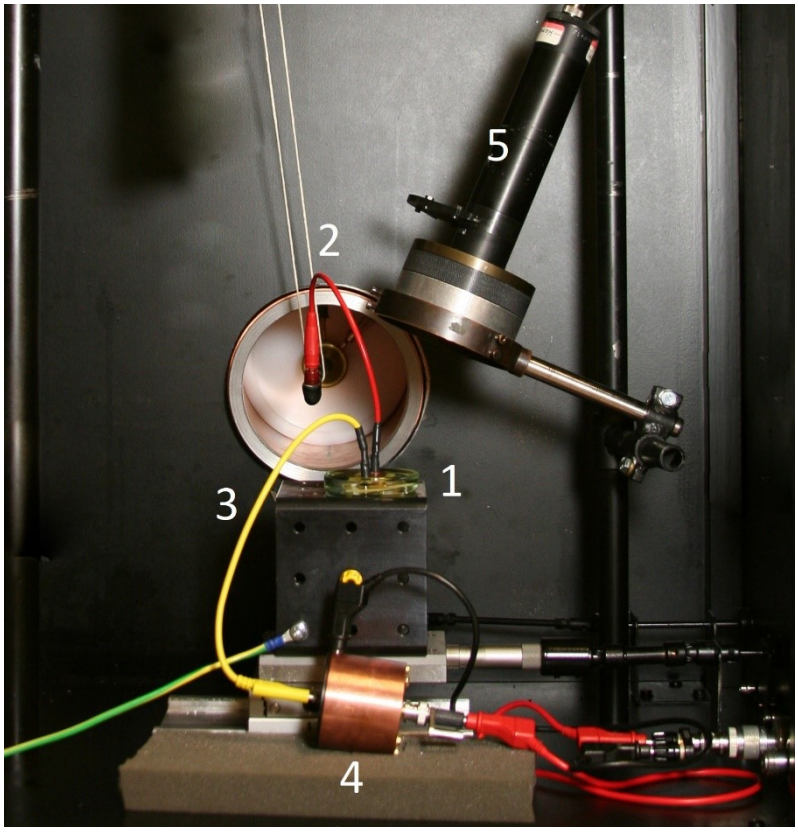

Figure 43 Inside measuring cabinet: 1) Test object, 2) HV connection, 3) Earth side of test object connected to measuring interface, 4) Resistive shunt, 5) Photomultiplier.

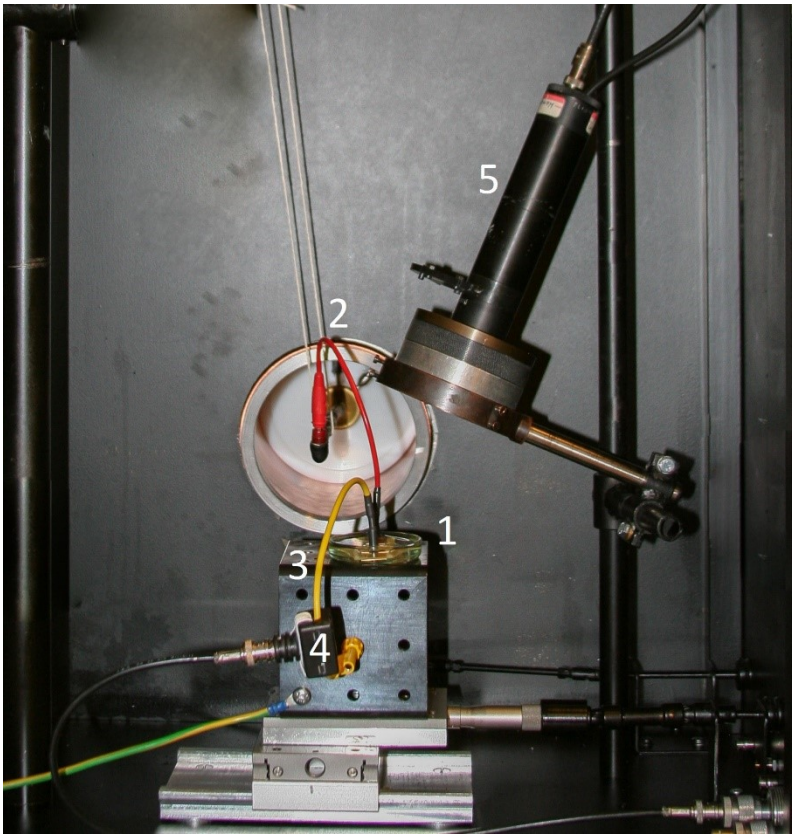

Figure 44 Inside measuring cabinet: 1) Test object, 2) HV connection, 3) Earth connection, 4) HFCT around the earth connection, 5) Photomultiplier.

7.2 Appendix II - Matlab Programs

ConnectAndRecieve.m:

Based on an example in the Yokogawa Matlab toolkit manual [31].

```
% Variables to be set
num = 20; % Number of triggers to record
text = 'text'; % Custom text for filename

% Choose USB as the connection interface, and input serial number
ret = mexDLComStart(7, 'SerialNumber');

% Set which terminals to collect data from
ret = mexDLSetTerm( 2, 1 );
if ret ~= 0
   ret = mexDLGetLastError;
   return;
end;

%Set timeout
ret = mexDLSetTimeout( 3000 );
if ret ~= 0
    ret = mexDLGetLastError;
    return;
end;

WaveData = 0; %WaveData is a variable where the data is stored

%Loop that stores "num" wavedata files
for i=1:num;

    % Start signal acquisition
    Ret = mexDLSend('sstart? 100');
    if Ret ~= 0
        Ret = mexDLGetLastError;
        return;
    end;

    [Ret,Buf,Size] = mexDLReceive( 10 );
    if Ret ~= 0
      Ret = mexDLGetLastError;
      return;
    end;

    % Receive DL data into WaveData matrix if a
    % signal is triggered
    if strcmp( deblank(Buf(1,:)), ':SST 0' ) == 1
        [Ret,WaveData] = mexDLGetWave(0);
        if Ret ~= 0
            Ret = mexDLGetLastError;
            return;
        end;

        d = datetime('today');
        fid = fopen(sprintf('WaveData_%s_%s_%d.txt',text,d,i),'wt');
        filename = fopen(fid);
        dlmwrite(filename,WaveData,'delimiter','\t');
        fclose(fid);
```

```
    end;

    % Set DL trigger mode to AUTO
    mexDLSend(':TRIG:MODE AUTO');
end;

%Close communication port
Ret = mexDLComEnd;
if ret ~= 0
    ret = mexDLGetLastError;
    return;
end;
```

ReadFiles.m:

```
clear all

task = input(['Available options:\n'...
    '1) Plot signal with/without averaged voltage\n'...
    '2) Plot signal compensated for average with/without voltage\n'...
    '3) Plot electrical vs optical\n'...
    '4) Plot wavelet analysis\n'...
    '5) Find PD pulses and plot scatter diagram\n'...
    '6) Extra: For manual control\n'...
    'Choose option 1 - 6: '], 's');

%Inputs to specify which files to be read
disp('Specify which files to be read');
text = input('Custom text: ','s');
d = input('Day (Ex: 05): ');
m = input('Month (Ex: Jan): ','s');
y = input('Year (Ex: 2018): ');
date = sprintf('%d-%s-%d',d,m,y);

if strcmp(task,'4')
    start = input('Choose wavedata no: ');
    stop = start;
else
    start = input('From wavedata no: ');
    stop = input('To wavedata no: ');
end
n = stop-start+1;

%Other variables
c = 1;
samples = 125000;

%Read files
for i = start:stop
    WaveData = dlmread(sprintf('WaveData_%s_%s_%d.txt',text,date,i),'\t');
    Ch1Data(:,c) = WaveData(:,1);
    Ch2Data(:,c) = WaveData(:,2);
    Ch3Data(:,c) = WaveData(:,3);
    %Ch4Data(:,c) = WaveData(:,4);
    c = c+1;
end

%Average of all measurements
Ch1Average = mean(Ch1Data,2);
Ch2Average = mean(Ch2Data,2);
Ch3Average = mean(Ch3Data,2);
%Ch4Average = mean(Ch4Data,2);

if strcmp('1',task) % Plot current with/without averaged voltage:
    av = input('Plot averaged voltage? 1-Yes/0-No :');

    figure;
    x = linspace(-2*10^-7,18*10^-7,samples); %Transform x-axis into time
    y = Ch3Data;
    plot(x, y) %Plot current measurements
    xlabel('Time in relation to voltage flank [s]')
    ylabel('Measured signal [V]')
```

```
    if av == 1
        yyaxis right
        z = Ch1Average;
        plot(x, z); %Plot averaged voltage
        %Set what x-axis timestamps to show
        xticks([-2*10^-7:2*10^-7:18*10^-7])
        ylabel('Averaged applied voltage [kV]')
    end

elseif strcmp('2',task)% Plot current compensated for average:
    av = input('Plot averaged voltage? 1-Yes/0-No :');
    a = input(['Choose wich of the averaged waveforms to plot: '...
        'From waveform no: ']);
    b = input('To waveform no: ');

    %All Ch3 measurements subtracted by average
    Ch3Corr = Ch3Data-Ch3Average;

    figure;
    x = linspace(-2*10^-7,18*10^-7,samples); %Transform x-axis into time
    y = Ch3Corr(:,a:b);
    plot(x, y);
    xlabel('Time in relation to voltage flank [s]')
    ylabel('Measured signal [V]')

    if av == 1
        yyaxis right
        z = Ch1Average;
        plot(x, z); %Plot averaged voltage
        xticks([-2*10^-7:2*10^-7:18*10^-7])
        ylabel('Averaged applied voltage [kV]')
    end

elseif strcmp('3',task) %Plot electrical vs optical:
    x = linspace(-2*10^-7,18*10^-7,samples); %Transform x-axis into time
    y = Ch3Data;
    z = Ch2Data;

    figure;
    subplot(2,1,1)
    plot(x,y)
    xlabel('Time in relation to voltage flank [s]')
    ylabel('Electrical [V]')

    subplot(2,1,2)
    plot(x,z)
    xlabel('Time in relation to voltage flank [s]')
    ylabel('Optical [V]')

elseif strcmp('4',task) %Wavelet analysis:
    wavelet = 'db8'; %Mother wavelet
    [c,l] = wavedec(Ch3Data,8,wavelet); % change for other than level 8
    approx = appcoef(c,l,wavelet);
    [cd1,cd2,cd3,cd4,cd5,cd6,cd7,cd8] = detcoef(c,l,[1 2 3 4 5 6 7 8]);
    a8 = wrcoef('a',c,l,wavelet,8);
    d8 = wrcoef('d',c,l,wavelet,8);
    d7 = wrcoef('d',c,l,wavelet,7);
    d6 = wrcoef('d',c,l,wavelet,6);

    subplot(5,1,1)
    plot(Ch3Data)
    ylabel('s')
```

```
    subplot(5,1,2)
    plot(a8)
    ylabel('a8')
    subplot(5,1,3)
    plot(d8)
    ylabel('d8')
    subplot(5,1,4)
    plot(d7)
    ylabel('d7')
    subplot(5,1,5)
    plot(d6)
    ylabel('d6')

elseif strcmp('5',task) %Finding PD size and position:
    %All Ch3 measurements subtracted by average
    Ch3Corr = Ch3Data-Ch3Average;
    %Remove all values less than 0.1 mV
    Ch3Corr(Ch3Corr < 0.1) = 0;
    Peaks = [];

    % For loop that finds all peaks w/locations, excludes peaks closer than
    % 100 ms to avoid registering the same PD pulse twice:
    for p = start:stop
    [pks,locs] = findpeaks(Ch3Corr(:,p),'MinPeakDistance',6250);
    Peaks(end+1:end+length(pks),:) = [pks locs];
    end
    % Samples converted into time and adjusted to time after switching
    Peaks(:,2)=Peaks(:,2)*0.016*10^-9-200*10^-9;
    % Plots the peaks in a scatter plot:
    figure;
    scatter(Peaks(:,2),Peaks(:,1))
    xlabel('PD position in relation to switching moment [s]')
    ylabel('PD amplitude [V]')

    % Extra program for comparing electrical, optical measurements with
    % detected PDs:
elseif strcmp('6',task)
    Ch3Corr = Ch3Data-Ch3Average;
    Ch3Corr(Ch3Corr < 0.1) = 0;
    Peaks = [];
    i = 1;
    while i ~= 0

    i = input('Measurement no (0 to end): ');

    if i ~= 0
        [pks,locs] = findpeaks(Ch3Corr(:,i),'MinPeakDistance',6250);
        Peaks = [pks locs];

        subplot(3,1,1)
        plot(Ch3Data(:,i));
        yyaxis left
        xlabel('Sample 0 to 125000')
        ylabel('Voltage measured with resistive shunt (V)')

        subplot(3,1,2)
        plot(Ch2Data(:,i));
        yyaxis left
        xlabel('Sample 0 to 125000')
        ylabel('PD measured with Photomultiplier (V)')

        subplot(3,1,3)
```

```
        scatter(Peaks(:,2),Peaks(:,1))
        title(sprintf('PD activity at %d flanks', n))
        xlabel('Position in relation to switching moment [s]')
        ylabel('Measured current (V)')
    else
        disp('Control ended');
    end
    end

else
    error('Not Available');
end
```